RESULTS AND DISCUSSION

4- RESULTS AND DISCUSSION

4.1. γ-Pyrone

4.1.1. Chemistry of New Derivatives of γ-Pyrone

4.1.1.1. Synthesis of Visnagin-9-sulphonic esters (IIa-e)

In the present investigation **(IIa-e)** were synthesized via treating visnagin 9-sulphonyl chloride[84] with cyclohexanol, cyclopentanol and appropriate phenol derivatives namely, 4-fluorophenol, 4-methoxy phenol and 4-nitrophenol in benzene in the presence of anhydrous potassium carbonate in relation to similar work[85-86].

The structure of **(IIa-e)** were confirmed by correct elemental analysis and spectroscopic data

IR spectra of compound **II** showed the enone absorption band at 1638 cm^{-1}, while GC-MS of compounds **II** showed the following data

GC-MS of compound	M^+ at m/z	abundance
IIb	378	(5%) $[C_{18}H_{18}O_7S]^{+\cdot}$
IIc	404	(40%) $[C_{19}H_{13}O_7SF]^{+\cdot}$
IId (c.f.Fig 1).	416	(4%) $[C_{20}H_{16}O_8S]^{+\cdot}$

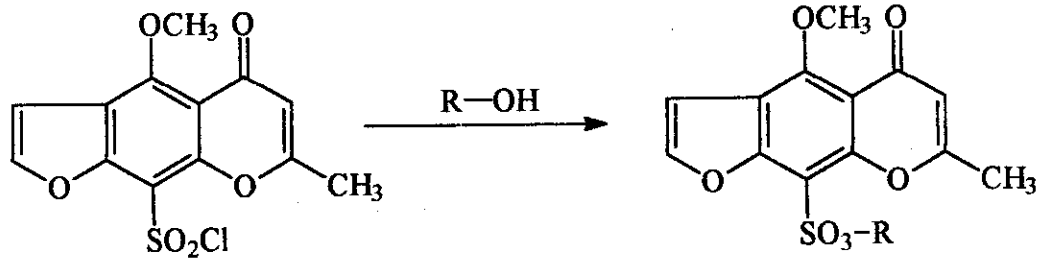

I **II**

R:
- **a,** Cyclohexyl
- **b,** Cyclopentyl
- **c,** 4-Fluorophenyl
- **d,** 4-Methoxyphenyl
- **e,** 4-Nitrophenyl

4.1.1.2. Mannich Reaction of derivatives II

When compound II was subjected to Mannich reaction using formaldehyde and 2^{ry} amine where Mannich base was prepared first to give compounds **(IIIa-i)**.

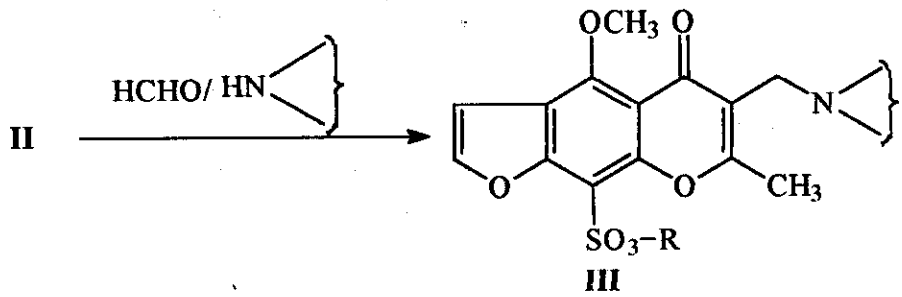

III

	R	N
a,	Cyclohexyl	Morpholinyl
b,	4-Fluorophenyl	Morpholinyl
c,	4-Nitrophenyl	Morpholinyl
d,	Cyclohexyl	Piperidinyl
e,	4-Fluorophenyl	Piperidinyl
f,	4-Nitrophenyl	Piperidinyl
g,	Cyclohexyl	Pyrolidinyl
h,	4-Fluorophenyl	Pyrolidinyl
i,	4-Nitrophenyl	Pyrolidinyl

The structure of **(III)** were confirmed by correct elemental analysis and spectroscopic data

IR spectra of both compounds **IIIa** and **IIIc** revealed the enone absorption band 1633-1634 cm^{-1}, the SO_2 absorption band at 1375-1368 cm^{-1} and 1087-1094 cm^{-1}.

^{1}H-NMR spectra of compounds **IIIb** and **IIIh** show the following signals at δ: 2.55, (m, 2H N-CH_2 ring 2^{ry} amine), 2.66 (s, N-CH_2 mannich methylene bridge), 3.6 (s, 3H O-CH_3), 7.2(d 1H C-3 furan ring), 7.35 (m, aromatic protons)and 7.70(d 1H C-2 furan ring) (Fig.2) is a representative example for the ^{1}H-NMR of compound (**IIIh**).

GC-MS of compound	M^+ at m/z	abundance
IIIa	491	(7%) $[C_{24}H_{29}NO_8S]^{+\cdot}$.
IIId	489	(87%) $[C_{25}H_{31}NO_7S]^{+\cdot}$.
IIIg	475	(5%) $[C_{24}H_{29}NO_7S]^{+\cdot}$

4.1.1.3. Reaction with hydroxylamine hydrochloride

When compound **II** reacted with hydroxyamine hydrochloride it gave o(sub)-6-hydroxy-4-methoxy-5-(4`-methyl-isoxazol-3-yl) benzofuran-7-sulphonates **(IV)**.

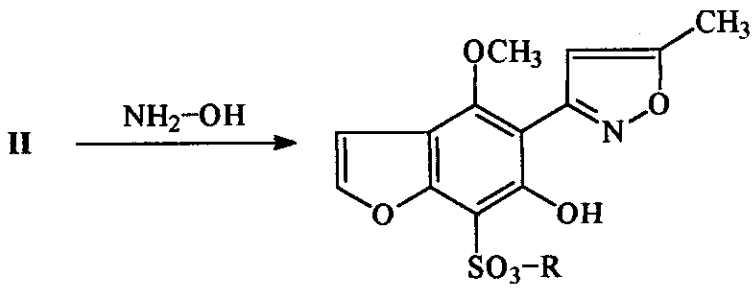

IV

R		R	
a,	Cyclohexyl	**d,**	4-Methoxyphenyl
b,	Cyclopentyl	**e,**	4-Nitrophenyl
c,	4-Fluorophenyl		

The reaction probably takes place according to the following mechanism c.f.**(Scheme 1).**

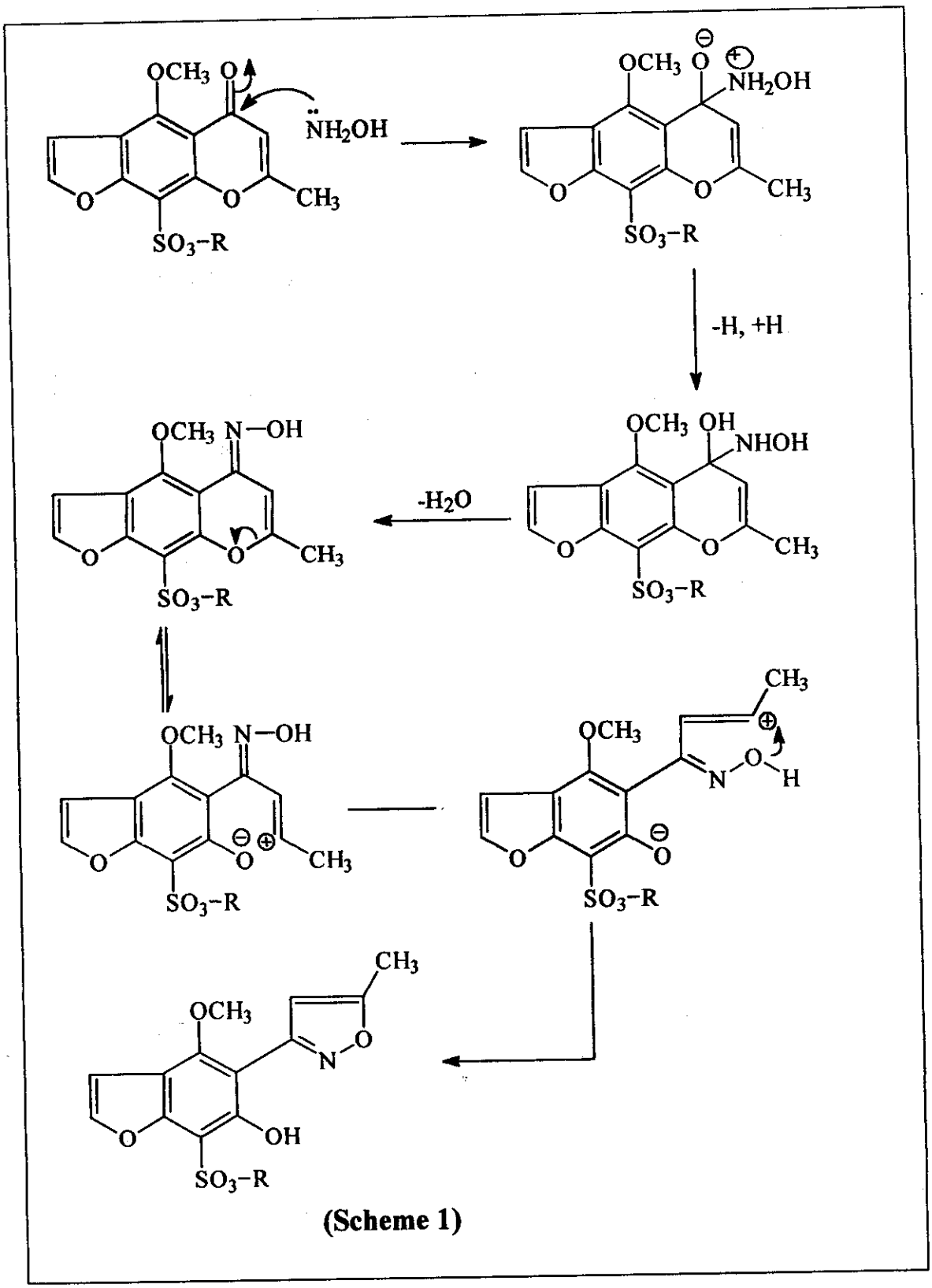
OCH3 O
NH2OH
CH3
SO3–R
OCH3 O NH2OH
-H, +H
OCH3 OH NHOH
-H2O
OCH3 N–OH
CH3
OCH3 N–OH
CH3
OCH3
N
O
H
CH3
OCH3
N
O
OH
SO3–R

(Scheme 1)

The structure of **(IV)** were confirmed by correct elemental analysis and spectroscopic data

FT-IR spectrum of compound **IVb** (Fig. 3) revealed the absence of enone absorption band and the presence of OH, C=N absorption bands at 3439 cm^{-1} and 1614 cm^{-1}.

^{1}H-NMR spectrum of compound **IVc** (Fig. 4) revealed the presence of the following signals at δ: 2.51 (s, 3H, CH_3 of isoxazole ring), 3.50 (br, 1H, OH), 4.31 (s, 3H, OCH_3), 6.19 (s, 1H, isoxaziole proton), 7.21 (m, 1H, olefinic proton), 7.33-7.48 (m, aromatic protons) and 7.6 (d, 1H, furan protons).

GC-MS of compound		M^+ at m/z	abundance
(Fig. 5).	**IVa**	407	(11%) $[C_{19}H_{21}NO_7S]^{+\cdot}$
	IVd	431	(14%) $[C_{20}H_{17}NO_8S]^{+\cdot}$
	IVe	446	(5%) $[C_{19}H_{14}N_2O_9S]^{+\cdot}$

4.1.1.4. Action of aromatic amines

It was reported that visnagin reacted with primary aliphatic amines but not secondary amines, with the opening of the γ-pyrone ring and the formation of enamine derivatives[87-88].

The author study, the reaction of **(II)** with different aromatic amine. All cases opening of the pyron ring without Shiff's base formation

[forming the corresponding o(aryl)-6-hydroxy-5-[1-(3-amino-aryl-but-2-en-1-one)]benzofuran-7-sulphonate (Va-k), this supported by the

[forming the corresponding o(aryl)-6-hydroxy-5-[1-(3-amino-aryl-but-2-en-1-one)]benzofuran-7-sulphonate (Va-k), this supported by the presence of a carbonyl and (NH, OH) absorption bands at 1719-1730 cm^{-1} and 3427 cm^{-1} in the FT-IR spectra of both derivatives (**Vc**) and (**Vi**) respectively as representative example (Fig. 6) is the FT-IR spectrum of compound (**Vc**).

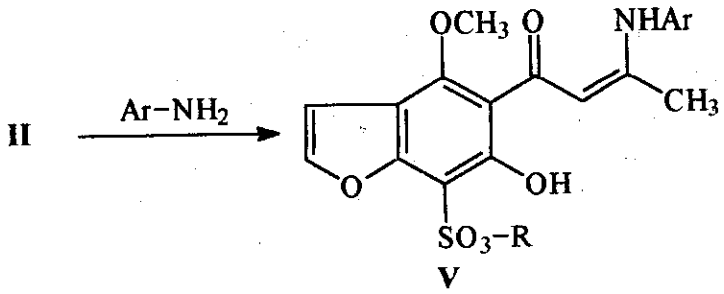

V

	R	Ar
a,	Cyclohexyl	Phenyl
b,	Cyclopentyl	Phenyl
c,	4-Fluorophenyl	Phenyl
d,	4-Nitrophenyl	Phenyl
e,	Cyclohexyl	4-Chlorophenyl
f,	Cyclopentyl	4-Chlorophenyl
g,	4-Fluorophenyl	4-Nitrophenyl
h,	4-Nitrophenyl	4-Methoxyphenyl
i,	Cyclohexyl	4-Nitrophenyl
j,	4-Fluorophenyl	4-Fluorophenyl
k,	4-Nitrophenyl	4-Nitrophenyl

The reaction probably takes place according to the following mechanism (c.f., Scheme 2).

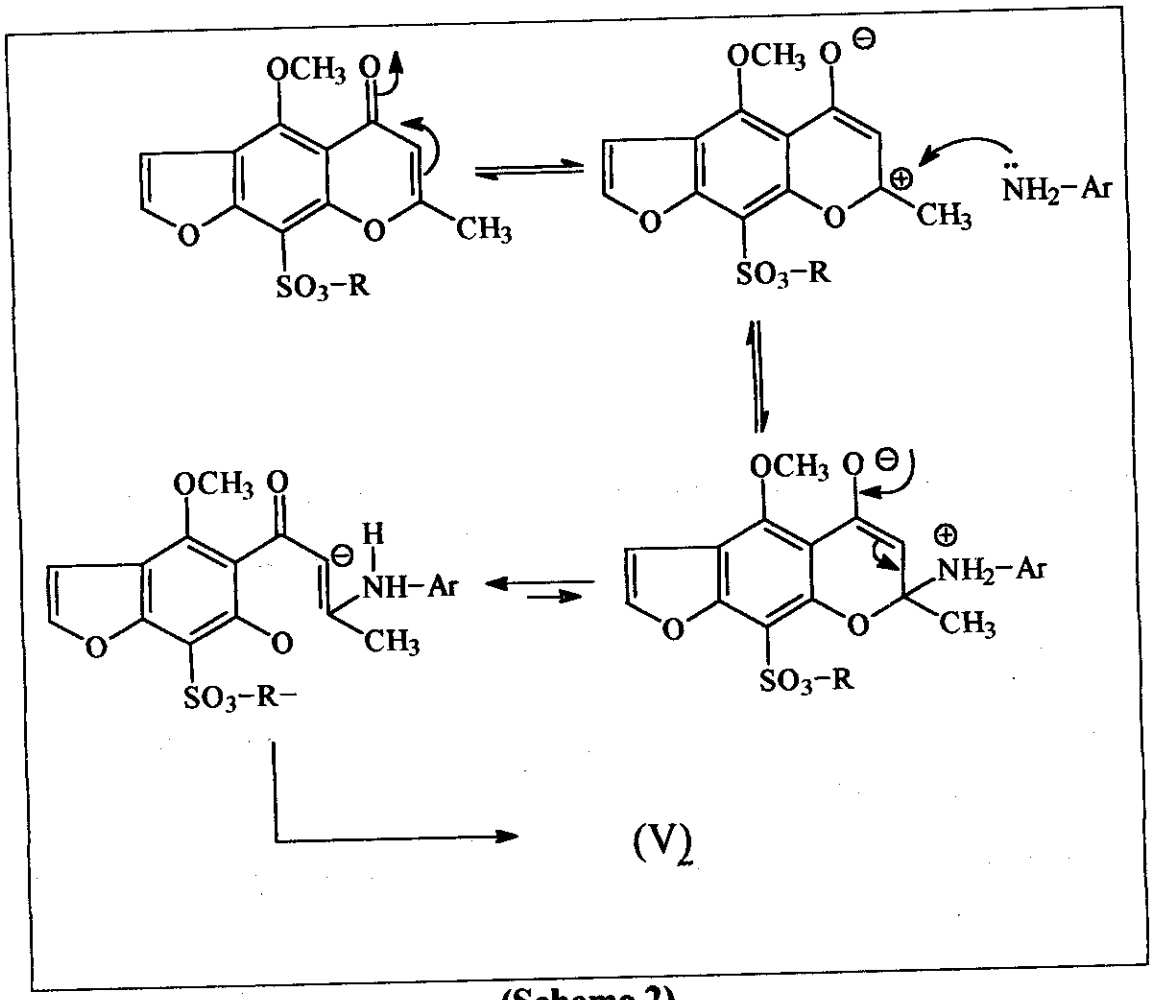

(Scheme 2)

The structure of (**V**) were confirmed by correct elemental analysis and spectroscopic data

^{1}H-NMR spectrum of compound **Vd** (Fig. 7) showed the following signals at δ ppm: 2.27 (s, 3H, CH_3), 4.31 (s, 3H, OCH_3), 6.27 (s, 1H, enone proton of the butenone side chain), 7.19-7.58 (s, 9H, aromatic protons), 7.37 (d, 1H, C-3 furan proton), 7.61 (d, 1H,C-2 furan proton).

^{1}H-NMR spectrum of compound **Vh** (Fig. 8) showed the following signals at δ ppm: 2.31 (s, 3H, CH_3), 3.51 (s, 3H, methoxy protons of NHAr), 4.27 (s, 3H, OCH_3 of the furocoumarin nucleus), 6.31 (s, 1H, enone proton of the butenone side chain), 7.14-7.53 (m, 8H, aromatic

protons), 7.30 (d, 1H, C-3 furan proton), 7.80 (d, 1H C-2, furan proton) and 8.61 (s, 1H, NH).

GC-MS of compound	M^+ at m/z	abundance
Va	486	(7%) $[C_{25}H_{27}NO_7S]^{+\cdot}$
Vb	471	(80%) $[C_{24}H_{25}NO_7S]^{+\cdot}$
(Fig. 9). **Vc**	498	(41%) $[C_{25}H_{20}NO_7SF]^{+\cdot}$

4.1.1.5. Action of 2ry cyclic amine on derivativs II

It was found that the NH of 2ry amine attack the enone of the pyran ring at locent 4 (1,4 Micheal addition) leading to the formation of 4-methoxy-7-methyl-7-(morpholino, pyrolidino or piperidino)-5-oxo-5H-furo[3,2-g][1]benzodihydropyran-9-sulphonate(**VIa-i**) without ring opening.

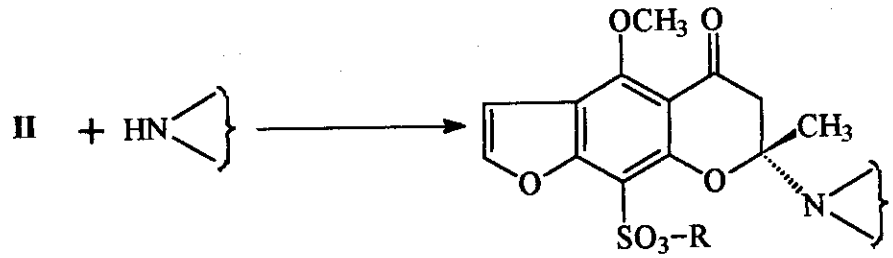

(VI)

R	N
a, Cyclohexyl	Morpholino
b, 4-Fluorophenyl	Morpholino
c, 4-Nitrophenyl	Morpholino
d, Cyclohexyl	Piperidino
e, 4-Fluorophenyl	Piperidino
f, 4-Nitrophenyl	Piperidino
g, Cyclohexyl	Pyrolidino
h, 4-Fluorophenyl	Pyrolidino
i, 4-Nitrophenyl	Pyrolidino

The reaction probably take place according to the following mechanism (Scheme 3).

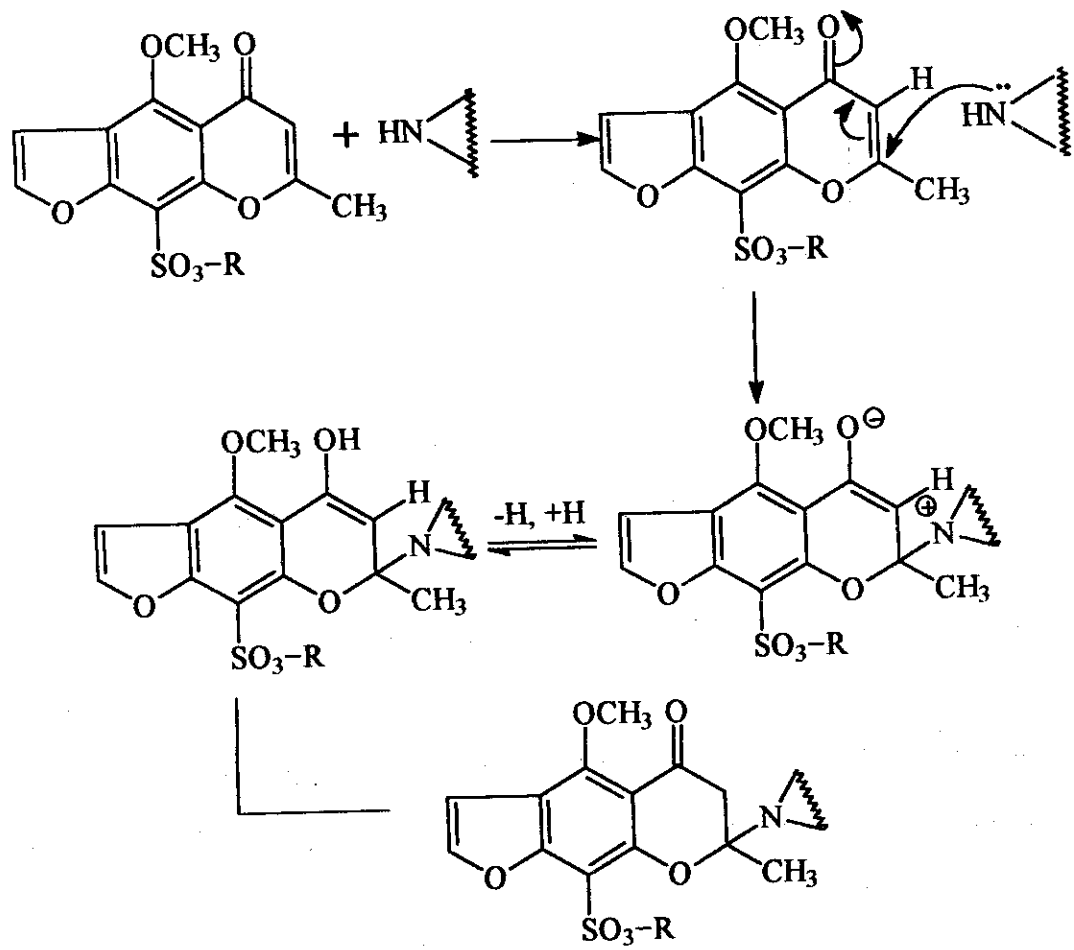

(Scheme 3)

The structure of (**VI**) were confirmed by correct elemental analysis and spectroscopic data

The disaperence of the double bond of the enone absorption band and the presence of the carbonyl absorption band at 1735 cm^{-1} in the IR spectra of both compounds **VIa** and **VId** is a good evidence of the 1,4-addition of the 2^{ry} amine at locent (4) of the enone without opening the pyran ring. Another evidence came from ^{1}H-NMR of both compound **VIa** (Fig. 10) and **VIh**.

^{1}H-NMR spectrum of compound **VIa** showed the following signals at δ ppm: 1.5-1.7 (m, 10H, cyclohexane protons), 2.48 (s, 3H, CH_3 at

4.1.1.6. The Action of hydrazines on derivativs II :

treating of compound **II** with hydrazines gave o(aryl)-6-hydroxy-4-methoxy-5-[5`-methyl-1H-1`-(methyl or phenyl)-pyrazolo-3-yl]benzo-furan-7-sulphonate **(VIIa-i).**

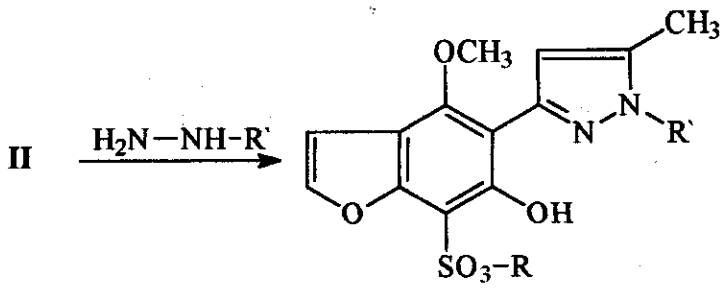

VII

	R	R`
a,	Cyclopentyl	H
b,	4-Fluorophenyl	H
c,	4-Nitrophenyl	H
d,	Cyclohexyl	Methyl
e,	4-Nitrophenyl	Methyl
f,	Cyclohexyl	Phenyl
g,	Cyclopentyl	Phenyl
h,	4-Fluorophenyl	Phenyl
i,	4-Nitrophenyl	Phenyl

The reaction probably takes place via the following mechanism (Scheme 4).

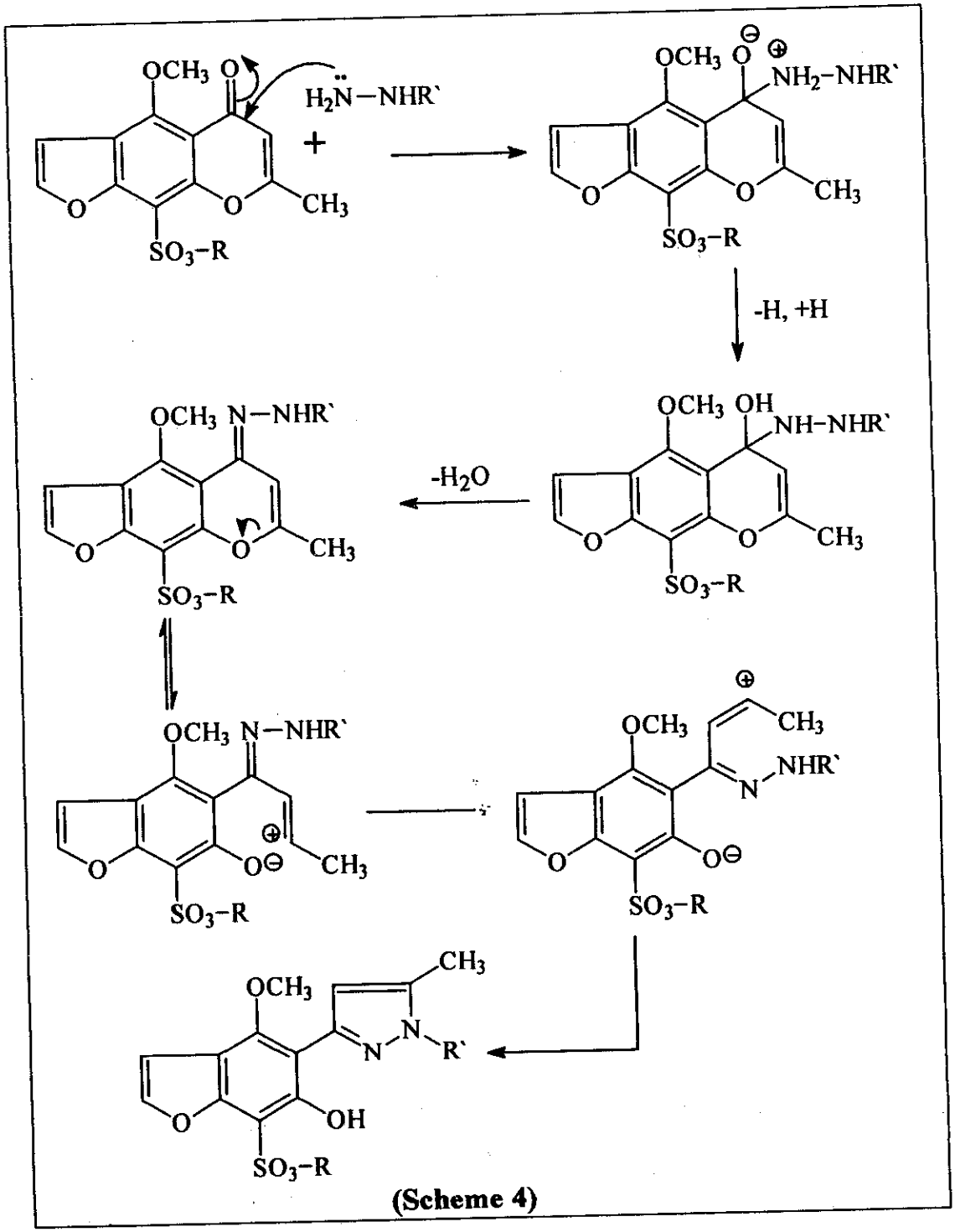
OCH3 O
H2N–NHR`
+
CH3
O
O
SO3–R
OCH3 O ⊖ ⊕
NH2–NHR`
-H, +H
OCH3 OH
NH–NHR`
-H2O
OCH3 N–NHR`
OCH3 N–NHR`
⊕
CH3
O⊖
OCH3
CH3
⊕
NHR`
N
OCH3
CH3
N
N
R`
OH

(Scheme 4)

The structure of **(VII)** were confirmed by correct elemental analysis and spectroscopic data

IR spectra of compounds **(VIIi)** showed the disappearance of the carbonyl group and the appearance of (OH) and (C=N) absorption bands at 3439 and 1614 cm^{-1}. (Fig. 12).

^{1}H-NMR spectrum of compound **VIIf** revealed the presence of the following signals at δ ppm: 1.4-1.7 (m, 11H, cyclohexyl protons), 2.50 (s, 3H, CH_3 of pyrazoline ring), 4.31 (s, 3H, OCH_3), 6.09 (d, 1H, pyrazoline proton), 7.12 (m, 5H, aromatic protons), 7.37 (d, 1H, C-3 furan proton) and 7.54 (d, 1H, C-2 furan proton).

^{1}H-NMR spectrum of compound **VIIg** revealed the presence of the following signals at δ ppm: 1.41-1.69 (m, 9H, cyclpentyl protons), 2.39 (s, 3H, CH_3 of pyrazoline ring), 4.31 (s, 3H, OCH_3), 6.10 (s, 1H, pyrazoline proton), 7.28-7.35 (m, 4H, aromatic protons), 7.32 (d, 1H, C-3 furan proton) and 7.61 (d, 1H, C-2 furan proton) (Fig. 13).

GC-MS of compound (Fig. 14).

	M^+ at m/z	abundance
VIIb	418	(4%) $[C_{19}H_{15}N_2O_6SF]^{+\cdot}$
VIIc	445	(5%) $[C_{19}H_{15}N_3O_8S^{+\cdot}]$
VIIe	459	(10%) $[C_{20}H_{17}N_3O_8S]^{+\cdot}$

4.1.2. Invitro disease-oriented primary antitumer Screening

In the routine stage screening[89], each agent is tested over a broad concentration range against every cell line in the current panel.

All lines are inoculated onto a series of standard 96-well microlitre plates on day 0, in the majority of cases at 20,000 cells/well, then pre incubated in absence of drug for 24 hours.

Tested agents are then added in five tenfold dilutions starting from the highest concentration, and incubated for further 48 hours. Following this, the cells are fixed in sitter, washed, and dried, sulforhodamine B(SRB), the bound stain is solubilized and measured spectrophotometrically on automatic plate readers.

The parameter used here is GI_{50} which is the $\log_{10}$ concentration at which the PG is + 50.

4.1.2.1 Discussion:

survey of literature on the pharmacological activities of γ-pyrone & α-pyrone[14,39-44] revealed on the discovery of agents, some of estrogenic and other anti-estrogenic activities, this prompted the author to make a correlation between the estrogen level and ovarian cancer also breast cancer because high level of estrogen induce and initiate cancer in the ovary & breast, so our aim is to study probability of use of such a anti-estrogenic profile as anticancer agent to treat ovarian & breast cancer.

Another criterion present in such structure profile which is its planarity or co planarity that serve & support fitting of molecule inside DNA double helix, and inter chelate DNA considered as a good evidence for our aimed vision.

To serve the target some considerations should be applied :

1- Introduce Nitrogen center[90] to facilitate intramolecular hydrogen bonding with the purine & pyridine bases of DNA (serious II & VII).

2- Induce chalcone moiety into the planer structure[91,92] (serious V) that contain also the nitrogen & OH centers that permit & enable the compound to insert it in the grooves of DNA double helix via strong hydrogen bonding to stop its unwinding and therefore stop replication & multiplication of cancer ions DNA molecule. (N. B. chelcone it self have anticancer activities).

3- Make inversion of the planner structure[93,94] into another more hydrophilic planner one (with changed configuration) as in serious IV that serve two purpose, the first is the planner structure, the second is the centers that permit hydrogen bonding, both facilitate insertion of the molecule in special manner onto DNA grooves.

4- Change the planner into Co-planner structure[95] via 1,4 Michael addition of secondary amine of the basic γ-pyrone skeleton to study the effect of changing planarity on the anticancer activity (serious VI).

Compound IVa showed antibreast cancer & no antiovarian cancer, while compound IIIi showed no antibreast cancer & antiovarian cancer (but not against all type of ovarian cancer).

This calumniated on that compound IIIa is less hydrophilic and hence we can got to the conclusion that breast cancer need less hydrophilic structure while ovarian need higher hydrophilic structure compound IVe showed both anti-ovarian cancer and anti-breast cancer against a wide variety of cell lines (more brouder against a large number of cancerous breast cell lines).

The insertion of a centers of hydrogen bonding will permit fitting of the molecule onto the grooves of double helix to prevent its unwinding.

Compound Vg showed anti-breast cancer with no activity against ovarian cancer, this meet with the result for compound IIIa, and support our previous conclusion that breast cancer need more hydrophilic & electrophilic characters. (openining of γ-prane will limits the anticancer activity but have no mentioned advantage on ovarian cancer).

Compound VIe showed potent and broad anticancer activities against large numbers of breast cancer and ovarian cancer cell lines, here we got to the conclusion that Coplanar structure is needed to enter the DNA grooves to exert it anticancer activity.

Compounds VIIb & VIIe showed potent antivarian cancer against a wide variety of ovarian cancer cell lines this meet with the results for compounds IV where the five membered & bicyclic system is essential for anti-ovarian cancer beside the hydrophilic & electrophilic structures.

Ovarian Cancer

Comp. No.	IGROVI	OVCAR-3	OVCAR-5	OVCAR-8	OVCAR-4	SK-OV-3
IIIa	-	-	-	-	-	-
IIIi	4.12^{E-05}	-	-	3.81^{E-05}	-	-
IVe	7.12^{E-05}	-	-	4.14^{E-05}	-	3.56^{E-05}
Vg	-	-	-	-	-	-
VIe	8.80^{E-05}	9.15^{E-05}	9.38^{E-05}	-	3.84^{E-05}	3.68^{E-05}
VIIb	9.48^{E-05}	9.38^{E-05}	-	6.18^{E-05}	6.38^{E-05}	3.68^{E-05}
VIIe	-	-	-	-	-	-

Breast Cancer

Comp. No.	MDA MB.231 ATTC	MCF-7	T-47D	NCI ADR-RES	HS-578T	MDA MB-435	MiDA-N	BT 549
IIIa	5.21^{E-05}	4.16^{E-05}	4.26^{E-05}	7.47^{E-05}	3.86^{E-05}	4.63^{E-05}	-	-
IIIi	-	-	-	-	-	-	-	-
IVe	-	8.16^{E-06}	6.14^{E-06}	-	8.56^{E-06}	3.41^{E-06}	2.76^{E-06}	8.17^{E-06}
Vg	6.21^{E-06}	-	2.45^{E-06}	2.76^{E-06}	-	2.75^{E-06}	-	-
VIe	6.27^{E-06}	-	6.68^{E-06}	2.48^{E-06}	-	2.64^{E-06}	2.58^{E-06}	-
VIIb	-	-	-	-	-	-	-	-
VIIe								

4.1.3. Antiestrogenic activities

Compound No.	% reduction in Uterine weight
Anstrnzole	21
IIIa	14
IIIi	13
Ive	19
Vg	20
VIe	21
VIIb	23
VIIe	28

All the tested compounds [83a] showed anti-estrogenic activities while compound Vg & VI showed nearly the same activitiws as instrazol, while both compounds VIIb& VIIehave higher activities than instrazol (VIIe is the more potent).

From the above mentioned data we can get the final conclusion that antiestrogenic activities is needed for antiovarian cancer while low antiestrogenic activites is needed for antibreast cancer, due to the high estrogen content in the ovaries than in the breast, breast is manly estrogen effected but ovaries is estrogen deponent origin .

4.1.3.1 Structural activity relationship:

- Highest antiestrogenic activities need:

Bicyclic ring system & oxazole or pyrazole opening of γ-pyrone or its reduction

4.2. α-Pyrone

4.2.1. Chemistry of New α-Pyrone Derivatives

The present investigation deals with the introduction of amino acid into different positions of furocoumarin aiming to study its chemistry and SAR in the medicinal chemistry.

The adopted synthetic design depend on selection of both 5-hydroxy furocoumarin derivatives (5-hydroxy bergapten **24a** and 5-hydroxy isopimpinellin **24b**), They are prepared by alkaline hydrolysis of visnagin and khellin to give visnaginone and khellinone, The latters were condensed with ethyl carbonate to give 5-hydroxybergapten and 5-hydroxyisopimpinellin, respectively .

4.2.1.1. Reaction of (24a,b) with methyl glycinate and/or methylalanine ester.

Treatment of both (**24a** and **24b**) with methyl glycinate and alanine methyl ester gave two reaction products, The first product were 4-methoxy-5-hydroxy-5-(N-amino acid methyl ester)-7Hfuro[3,2-g] benzopyran-7-one **VIIIa,c** and 4,9-dimethoxy-5-hydroxy-5-(N-amino acid methyl ester)-7Hfuro[3,2-g]benzopyran-7-one **VIIIb,d**.

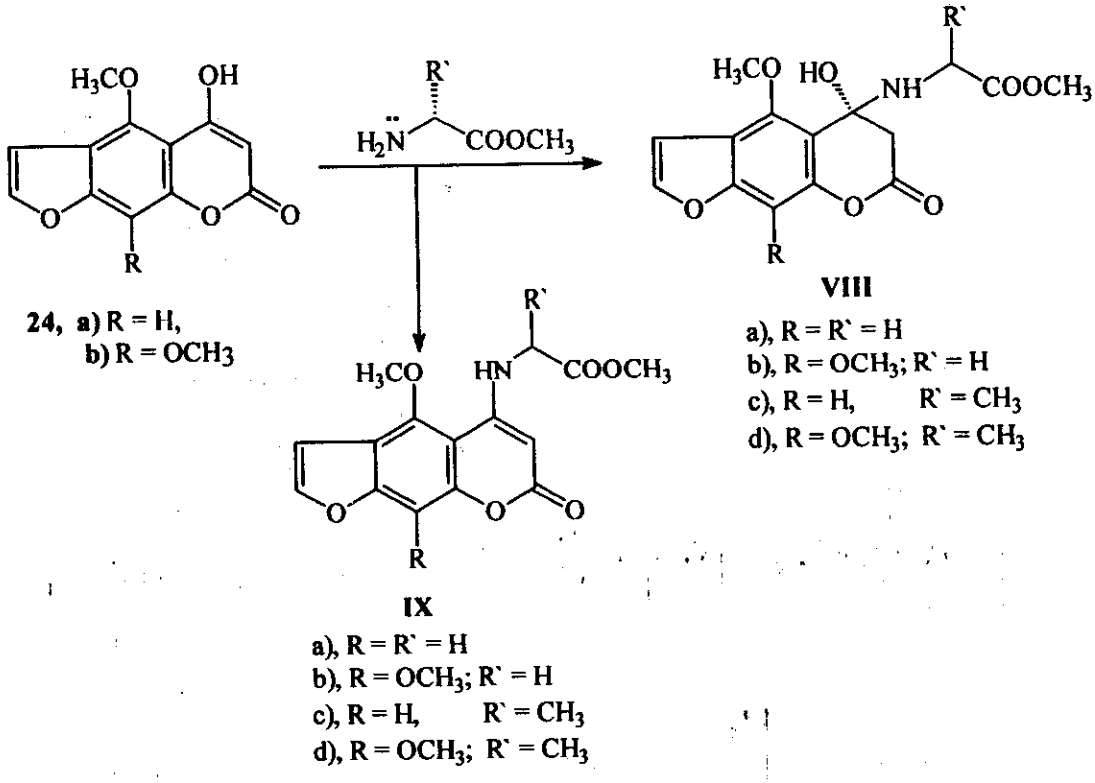

24, a) R = H,
b) R = OCH_3

VIII

a), R = R` = H
b), R = OCH_3; R` = H
c), R = H, R` = CH_3
d), R = OCH_3; R` = CH_3

IX

a), R = R` = H
b), R = OCH_3; R` = H
c), R = H, R` = CH_3
d), R = OCH_3; R` = CH_3

These derivatives formed by the 1,4-addition of the NH_2 of amino acid methyl ester on the enone system of the furocoumarin (c.f., proposed mechanism in Scheme 5).

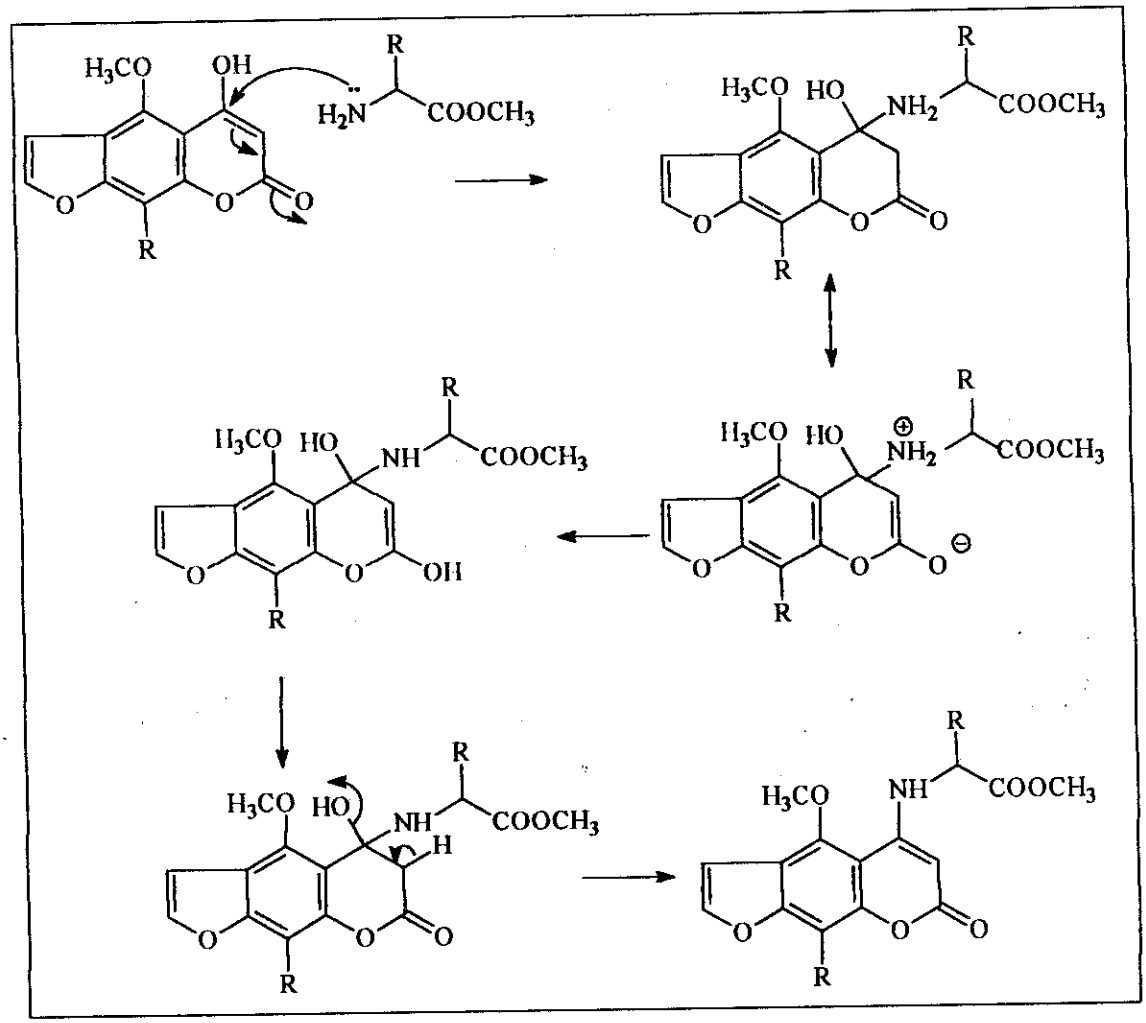

(Scheme 5)

The second derivatives were 4-methoxy-5-(N-amino methyl ester)-7H-furo[3,2-g]benzopyran-7-one **IXa,c** and 4,9-dimethoxy-5-(N-amino methyl ester)-7H-furo[3,2-g]benzopyran-7-one **IXb,d**, these derivative were formed probably by the removal of a molecule of water from derivative **VIII**.

The structure of **(VIII)** was confirmed by correct elemental analysis and spectroscopic data

FT-IR of compound **VIIIa** showed the disappearance of the enone absorption band and the presence of the following absorption bands 3427 cm^{-1}(OH), 3242 cm^{-1} (NH)and 1719 cm^{-1} (C=O) (Fig. 15).

^{1}H-NMR of compound (**VIIIa**) (Fig. 16) revealed the presence of the following peaks at δ ppm 2.31 (s, 2H, CH_2 protons of the pyran ring), 2.51 (s, 2H, CH_2COO), 3.39 (s, 3H, protons of methyl ester), 4.18 (s, 3H, OCH_3), 6.11 (s, 1H, NH), 6.6 (s, 1H, OH), 7.23 (d, 1H, C-3 furan proton), 8.41 (d, 1H, C-2 furan proton).7.1 (1 H aromatic).

GC-MS of compound (**VIIIb**) revealed $M^{+\cdot}$+1 at m/z 352 (71%) [$C_{16}H_{17}NO_8$] (Fig. 17).

The structure of (**IX**) was confirmed by correct elemental analysis and spectroscopic data

FT-IR of compound **IXa** still confirms the presence of the enone absorption band at 1668 cm^{-1}.

^{1}H-NMR of compound (**IXd**) showed the following peaks at δ ppm 2.31 (d, 3H, CH-$\underline{CH_3}$), 2.51 (m, 1H, N-CH), 3.31 (s, 3H, protons of methyl ester), 4.31 (s, 6H, OCH_3), 5.25 (s, 1H, NH), 6.21 (s, 1H, enone), 7.51 (d, 1H, C-3 furan proton), 8.19 (d, 1H, C-2 furocoumarin) (Fig. 18).

GC-MS of compound (**IXb**) revealed $M^{+\cdot}$ at m/z 333 (8%) [$C_{16}H_{15}NO_7$].

GC-MS of compound (**IXc**) revealed $M^{+\cdot}$ at m/z 317 (8%) [$C_{16}H_{15}NO_6$]

4.2.1.2. Reaction of bromo derivatives with amino acid esters

It was also aimed to introduce the amino acid ester at locent 6- and retaining the hydroxy enone profil of the pyran ring interact, to obtain

that we introduce for the first time the use of N,N-dibromohydentoin as a selective agent that make nuclear bromination at locent 6.

The bromo derivatives **Xa,b** treated with the amino acid ester to give the required structure profil (**XIa-d**).

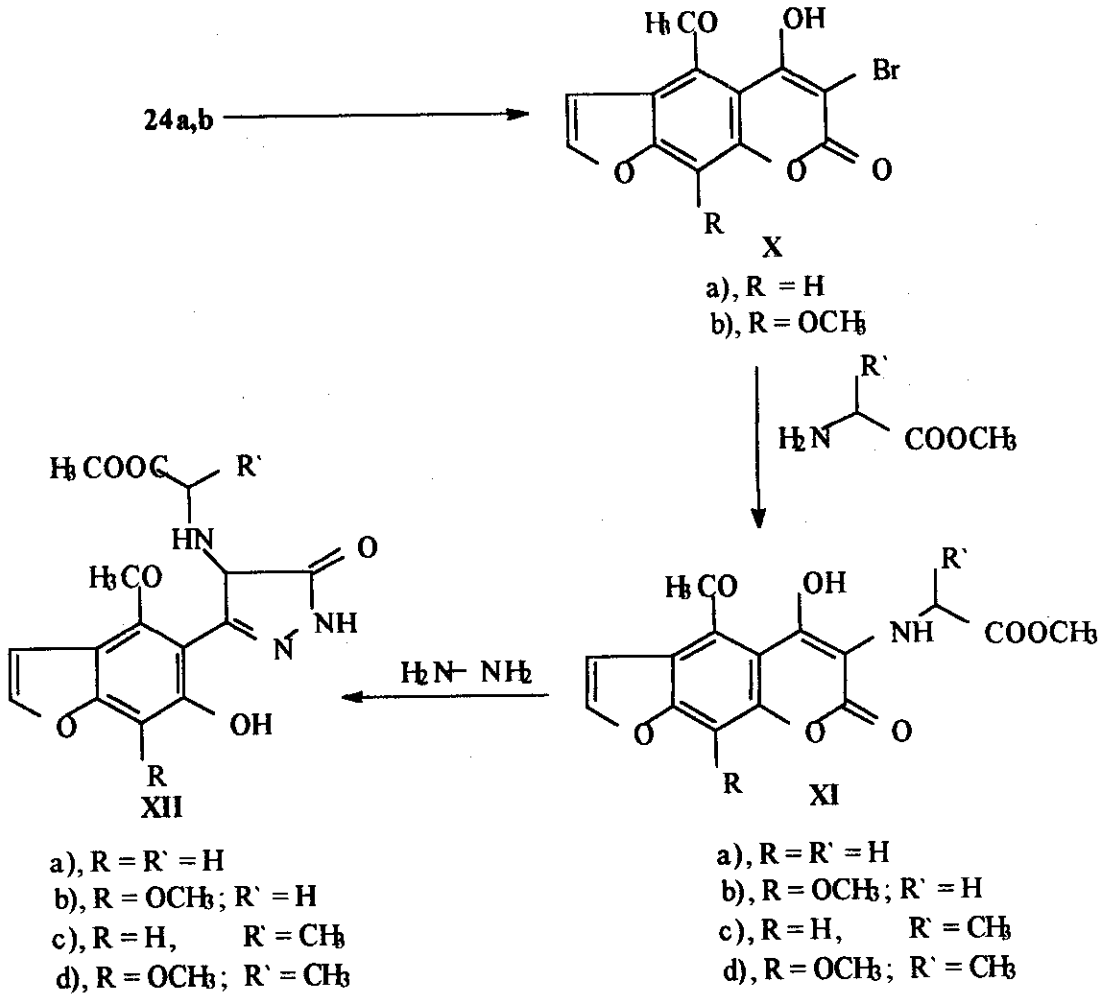

a), R = R` = H
b), R = OCH_3; R` = H
c), R = H, R` = CH_3
d), R = OCH_3; R` = CH_3

a), R = R` = H
b), R = OCH_3; R` = H
c), R = H, R` = CH_3
d), R = OCH_3; R` = CH_3

The presence of the intact enone was confirmed by the presence of the enone absorption band at 1661 cm^{-1} in the FT-IR of compound **XIb**.

^{1}H-NMR of compound (**XId**) showed the following peaks at δ ppm 2.27 (s, 3H, CH_3 of amino acid), 2.61 (m, 1H, CH of amino acid), 3.37 (s, 3H, $COOCH_3$), 4.3 (s, 6H, OCH_3), 6.17 (s, 1H, NH), 7.13 (d, 1H, C-3 of furocoumarin), 7.74 (d, 1H, C-2 furocoumarin) (Fig. 19).

GC-MS of compound (**XIa**) revealed M^+ at m/z 319 (3%) [$C_{15}H_{13}NO_7$].

GC-MS of compound (**XId**) revealed M^+ at m/z 363 (7%) [$C_{17}H_{17}NO_8$] (Fig. 20).

4.2.1.3. Reactions of XI with hydrazine hydrate

Treating compounds **XI**, with hydrazine hydrate afforded the corresponding 6-hydroxy-4-methoxy-5-[4`-(amino acid methyl ester)-1H-pyrazol-5-one-3-yl]benzofuran and 6-hydroxy-4,7-methoxy-5-[4`-(amino acid methyl ester)-1H-pyrazol-5-one-3-yl]benzofuran **(XIIa-d)**.

The reaction probably takes place via the following mechanism **(Scheme 6).**

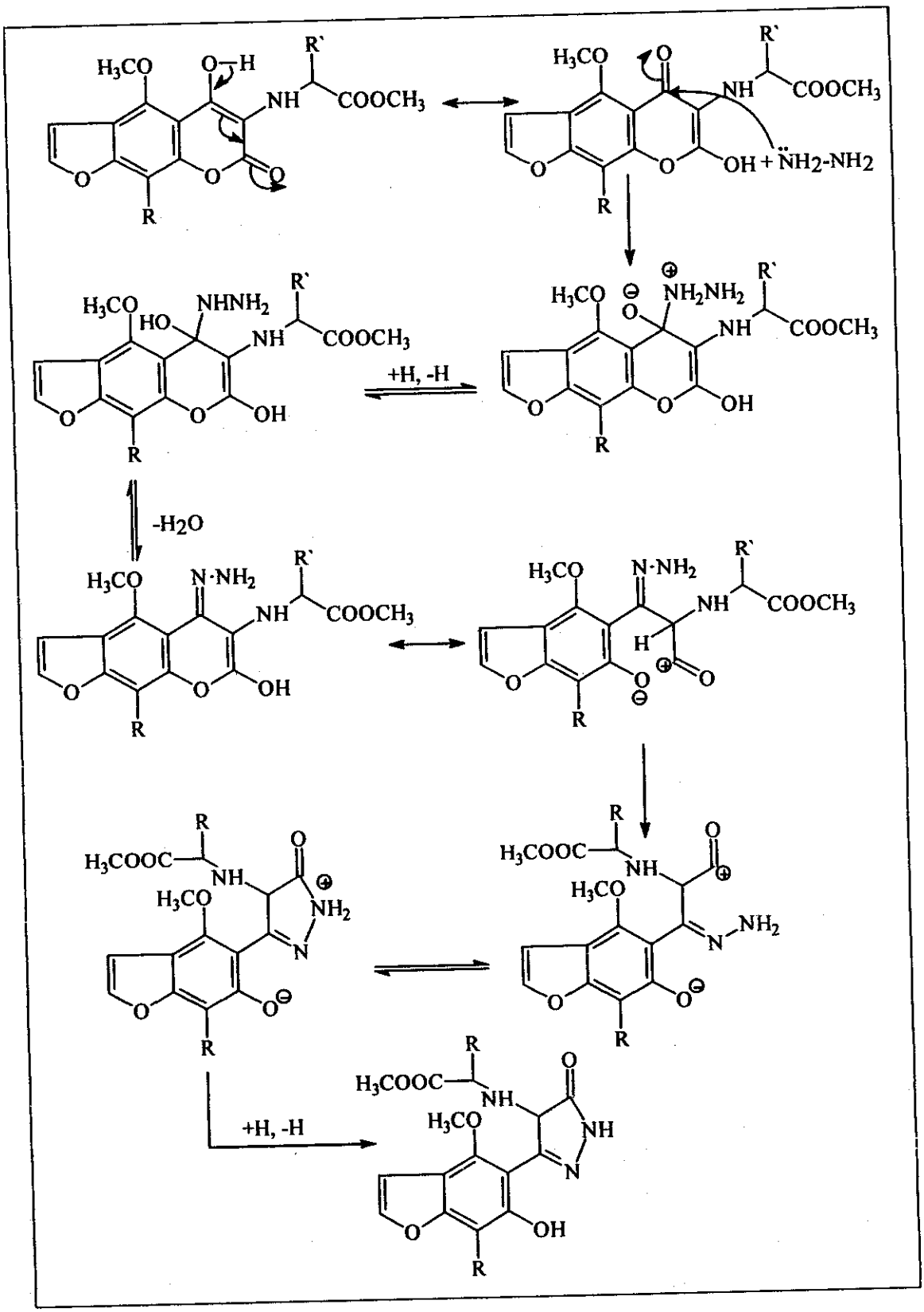
H3CO
O
H
NH
COOCH3
R`
R
O
OH + NH2-NH2
NHNH2
HO
+H, -H
-H2O
N·NH2
H3COOC
NH2
N

(Scheme 6)

The structure of **(XII)** was confirmed by correct elemental analysis and spectroscopic data

FT-IR of compound **(XIIa)** showed the following absorption bands at, 3423 cm^{-1} (OH), 3218 cm^{-1} (NH), 1719 cm^{-1} (C=O).

^{1}H-NMR of compound **(XIId)** showed the following peaks at δ ppm 2.11 (d, 3H, CH_3 of amino acid), 2.41 (m, 1H, CH of amino acid), 2.57 (s, 1H, pyrazolone), 3.17 (s, 1H, OH), 3.51 (s, 1H, NH), 4.31 (s, 6H, OCH_3), 6.71 (s, 1H, NH), 7.31 (d, 1H, C-3 of furocoumarin), 7.91 (d, 1H, C-2 furocoumarin) (Fig. 21).

GC-MS of compound	M^+ at m/z	abundance
(XIIb)	363	(3%) $[C_{16}H_{17}N_3O_7]$.
(XIIc)	347	(3%) $[C_{16}H_{17}N_3O_6]$
(XIId)	377	(8%) $[C_{17}H_{19}N_3O_7]$.

4.2.1.4. Reactions of the chloroformyl furocoumarin with amino acids

It was aimed to introduce the amino acid moiety at locent (5) and building the pyrazoline ring on the intack pyran ring (without neither opening the pyran ring nor reduction of its double bond).

The adopted synthetic pathway to construct such chemical profile based on that compound **(XIII)** have the availability of both chlorine atom utilized in introduction of amino acid (locent 5) and the formyl group at locent 6 that utilize to build the pyrazolone fused ring system by the aid of carbonyl group at locent (7).

Derivative **XIII** with the corresponding amino acid ester give the following compounds: 4-methoxy-5-(amino acid methyl ester)-6-formyl-7H-furo[3,2-g][1]benzopyran-7-one and 4,9-dimethoxy-5-(amino acid methyl ester)-6-formyl-7H-furo[3,2-g][1]benzopyran-7-one (**XIV**) where the amino acid methyl ester enter in position (5) and the formyl group still present at locent (6) that will be utilize in building the fused pyrazoline ring system.

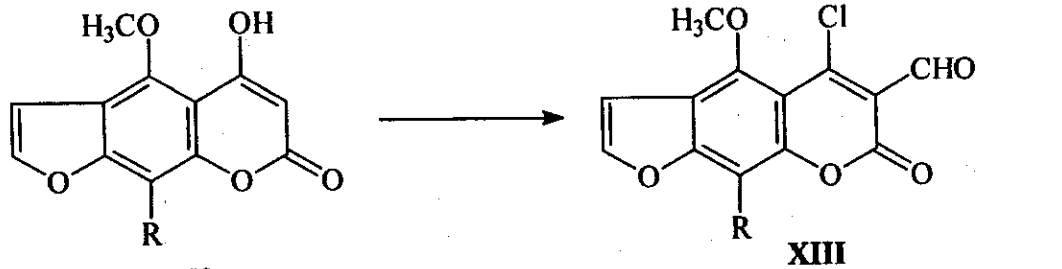

a), R = H
b), R = OCH_3

XIII
a), R = H
b), R = OCH_3

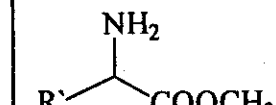

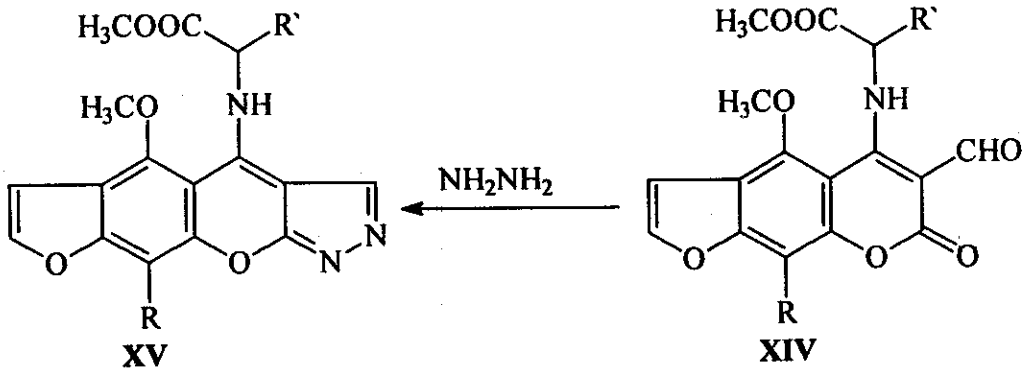

XV
a), R = R` = H
b), R = OCH_3; R` = H
c), R = H, R` = CH_3
d), R = OCH_3; R` = CH_3

XIV
a), R = R` = H
b), R = OCH_3; R` = H
c), R = H, R` = CH_3
d), R = OCH_3; R` = CH_3

Structural elucidation of derivative **XIV** revealed the following data , IR, ^{1}H-NMR and MS spectra.

IR spectrum of compound **XIVc** showed the following absorption bands at 3323cm^{-1}(NH), 1787 cm^{-1} (CHO) and at 1730 cm^{-1}(C=O).

^{1}H-NMR spectrum of compound (**XIVc**) revealed the following peaks at δ ppm 2.31 (d, 3H, CH_3 of amino acid), 2.61 (m, 1H, CH), 3.47 (s, 3H, $COOCH_3$), 4.23 (s, 3H, OCH_3), 6.17 (s, 1H, NH), 7.28 (s, 1H, Ar-H), 7.46 (d, 1H, C-3 of furocoumarin), 8.31 (d, 1H, C-2 furocoumarin), 9.12 (s, 1H, CHO) (Fig. 22).

GC-MS of compound	M^+ at m/z	abundance
(XIVb)	361	(5%) [$C_{17}H_{15}NO_8$].
(XIVd) (Fig. 23)	375	(4%) [$C_{18}H_{17}NO_8$]

4.2.1.5. Reactions of derivatives XIV with hydrazine hydrate

Treating derivatives **XIV**(a-d) with hydrazine hydrate yeilded the corresponding 4-methoxy-5-(amino acid methyl ester)-7H-furo[3,2-g][1]benzopyran[7,6-b]pyrazoline-7-one and 4,9-dimethoxy-5-(amino acid methyl ester)-7H-furo[3,2-g][1]benzopyran[7,6-b]pyrazoline-7-one (**XV**), where the hydrazine hydrate condensed with the CHO forming these derivatives.

IR spectrum of compound **XVc** showed the following absorption bands at 3481 cm^{-1} (NH)and 1732 cm^{-1} (C=O).

^{1}H-NMR spectrum of compound (**XVa**) showed the following peaks at δ ppm 3.31 (s, 2H, CH_2), 3.41 (s, 3H, $COOCH_3$), 4.97 (s, 1H, NH), 7.12 (s, 1H, pyrazoline proton), 7.3 (d, 1H, C-3 furan proton), 7.71 (d, 1H, C-2-furan proton).

GC-MS of compound (**XVa**) it showed M^+ at m/z 327 (5%) [$C_{16}H_{13}N_3O_5$].

GC-MS of compound (**XVb**) (Fig. 24) showed M^+ at m/z 357, [$C_{17}H_{15}N_3O_6$]

4.2.2. Invitro disease-oriented primary antitumer screen:

The α-pyrone compounds are screened as in the case of γ-pyrone

4.2.2.1. DISCUSSION

The aim of the present rationalized biological screening based on a strong biological rational adopted for the synthetic strategies involved in these work as follow:

1)- Studying replacement of γ-pyrone by α-pyrane pattern on both the antibreast
cancer and antiovarian cancer.

2)- Introduction amino acids in deferent positions that facilitate groove fitting and hydrogen bonding interchelation.

3)- Construction of a structure profile containing bicyclic system, co-planer pyrazolone and amino acid moiety, to study the variations of these factors on the anticancers activities against both breast & Ovary cancer (N.B. this structure profile contain a centers for hydrogen bonding).

4)- Discussing the effect of introducing both amino acid center beside a formyl moiety that many involved in the direct formulation of malignant.

Conclusions

Compounds VIIIc showed anti breast cancer against wide types of all lines, with no anti ovarian cancer, while compounds XIb showed anti overian cancer against a wide types of all cell line with no antibreast cancer. So we got to the conclusion that α-pyrone is essential for antibreast cancer there amino acid have no role except its to be involved hydrogen bonding ability.

Another good evidence that support the previous conclusion comes from the broad & potent antiovarian cancer activities with no antibreast cancer obtained for compound XIc.

Compound XIId showed an antioverian cancer with also no detected antibreast cancer, this lead to that bicyclic and high electrophilic & electrophilic charucter is essintial for the antiovarian cancer activity as previously studied for γ-pyrone.

Compound XIVc have no anticancer activity against breast and ovarian cancer so our aim by add formyl group was failed to more formylation of DNA, because the formyl group is firmly attached to the molecule and not liable to be involved in biochemical reaction.

Addition of a fused ring system (tetracyclic planner structure profile) lead to maximize & broads both the antibreast cancer & antioverian cancer.

This due to the fitting of the tetracyclic structure its DNA grooves, and its ability to DNA chelation due to the amino acid and tetracyclic ring system.

4.2.2.2. Structural activity relationship

We can got to the following final conclusion points:

- α-Pyrone is essintial for the antiovarian cancer, while its reduced form is essential for antibreast cancer where amino acid have here no role except its ability to be involved in hydrogen bonding.

- The structure proofil constitute a bicyclic ring system (open α-pyrone) with a higher electrophilic and hydrophilic characters is essential for the antiovarian cancer.

-Formyl group feinted to formylate cancerous DNA as previously aimed, due to into high covalent bonded characters to the α-pyrone skeleton.

- Tetracyclic ring system increase both antioverian cancer and antibreast cancer.

Ovarian Cancer

Comp. No.	IGROVI	OVCAR-3	OVCAR-5	OVCAR-8	OVCAR-4	SK-OV-3
VIIIc	-	-	-	-	-	-
IXb	3.84^{E-08}	4.18^{E-08}	-	2.93^{E-05}	-	-
XIc	3.84^{E-05}	-	5.89^{E-05}	9.40^{E-05}	-	9.15^{E-05}
XIId	-	7.66^{E-06}	1.30^{E-05}	7.66^{E-06}	9.72^{E-06}	8.09^{E-06}
XIVc	-	-	-	-	-	-
XVd	9.34^{E-05}	-	8.94^{E-06}	9.23^{E-06}	5.49^{E-06}	-

Breast Cancer

Comp. No.	MDA MB.231 ATTC	MCF-7	T-47D	NCI ADR-RES	HS-578T	MDA MB-435	MiDA-N	BT 549
VIIIc	-	6.18^{E-08}	2.57^{E-05}	-	3.74^{E-05}	-	2.68^{E-05}	2.47^{E-06}
IXb	-	-	-	-	-	-	-	-
XIc	-	-	-	-	-	-	-	-
XIId	-	-	-	-	-	-	-	-
XIVc	-	-	-	-	-	-	-	-
XVd	-	2.57^{E-05}	3.68^{E-05}	-	6.46^{E-06}	-	7.77^{E-08}	-

4.2.3. Antiestrogenic activities

4.2.3.1. Results:

Compound	% Reduction in utrine weight
Anstrozole	21
VIIIa	9
VIIIc	12
IXb	13
IXd	18
XIa	14
XIc	16
XIId	18
XIVc	17
XV	13

All the tested compound showed Antiestrogenic activities and the most potent were compounds **IXd** and **XIId**.

Compounds VIIIc, IXb, XIa and XIc showed moderate antiestrogenic activities, while compounds IXd, XIId and XIVc and XV showed highest antiestrogenic activities.

This supports the previously attained conclusion with γ-pyrone that higher antiovarian cancer needs high antiesterogenic activities while antibreast cancer does not need such property.

4.2.3.1 Structural activity relationship

- Intact tricyclic α-pyrone profile showed moderate antiestro-genic activities.
- The highest estrogenic activities need.
- Formyl group at locent 6
- Tetracyclic planner ring system

Oleanolic acid Reactions

4.3.1. Chemistry

The molecule used in the previous study was glycrhetic acid (contain 11-one & 30 COOH) that oxidized to the 3 keto glycrhetic acid and 3 keto methyl glycyrhetate, both reacted with different patterns of substituted aromatic aldehydes in alkaline medium (30% alc. KOH). The corresponding benzylidine, α-hydroxysubstituted benzyl and α-ethoxy substituted benzyl derivatives (linked to C-2 of the olean nucleus) were obtained depending on the type of aldehyde used (according to the substitution pattern).

4. 3.1.1.Aldol condensation of some new models of triterpenoids

The aim of the present work is to study the effect of the following factors on the mechanism of aldol condensation and the type of reaction products.

a)- Removing 11 oxo function.

b)- Replacing C-30 carboxyl with C-28 one.

c)- Introducing a CH_3 at the C-1 of olean which servs in two purposes. The first was that provide steric hindrance in the intermediate resonance stabilized anion transition state which may contribute in the production of abnormal non expected novel products which may possess varied pharmacological activities; The second is that the methyl groups at C-1 may increases the anti-inflammatory activities.

To varify the above mentioned factors the author select oleanolic acid which is a bio isoester of glycyrhetic acid[83b] used in the previous study which is isolated

from olive trees. Oleanolic acid contain no keto group at locent 11 and contain C-28 carboxyl function. This main study began with D. H. R. Barton and continued with others[96-108]

To introduce the methyl function the author adopted certain synthetic design pathway depending firstly on protection the C-28 carboxylic group of oleanolic acid as methyl ester via treating oleanolic acid with diazomethane to obtaine methyl oleanolate **XVI**, The 3β-ol of methyl oleanolate was converted to the 3-oxo function via oxidation of (**XVI**) with killian's solution to obtain 3-keto-methyl oleanolate **XVII**.

The adopted rationalized synthetic design depending on treating **XVII** with DDQ (high potential oxidizing quinone) to introduce the double bond at locent Δ^1, the product obtained was Δ^1-3-ketomethyl oleanolate **XVIII**,

The structure was confirmed by correct elemental analysis and spectroscopic data

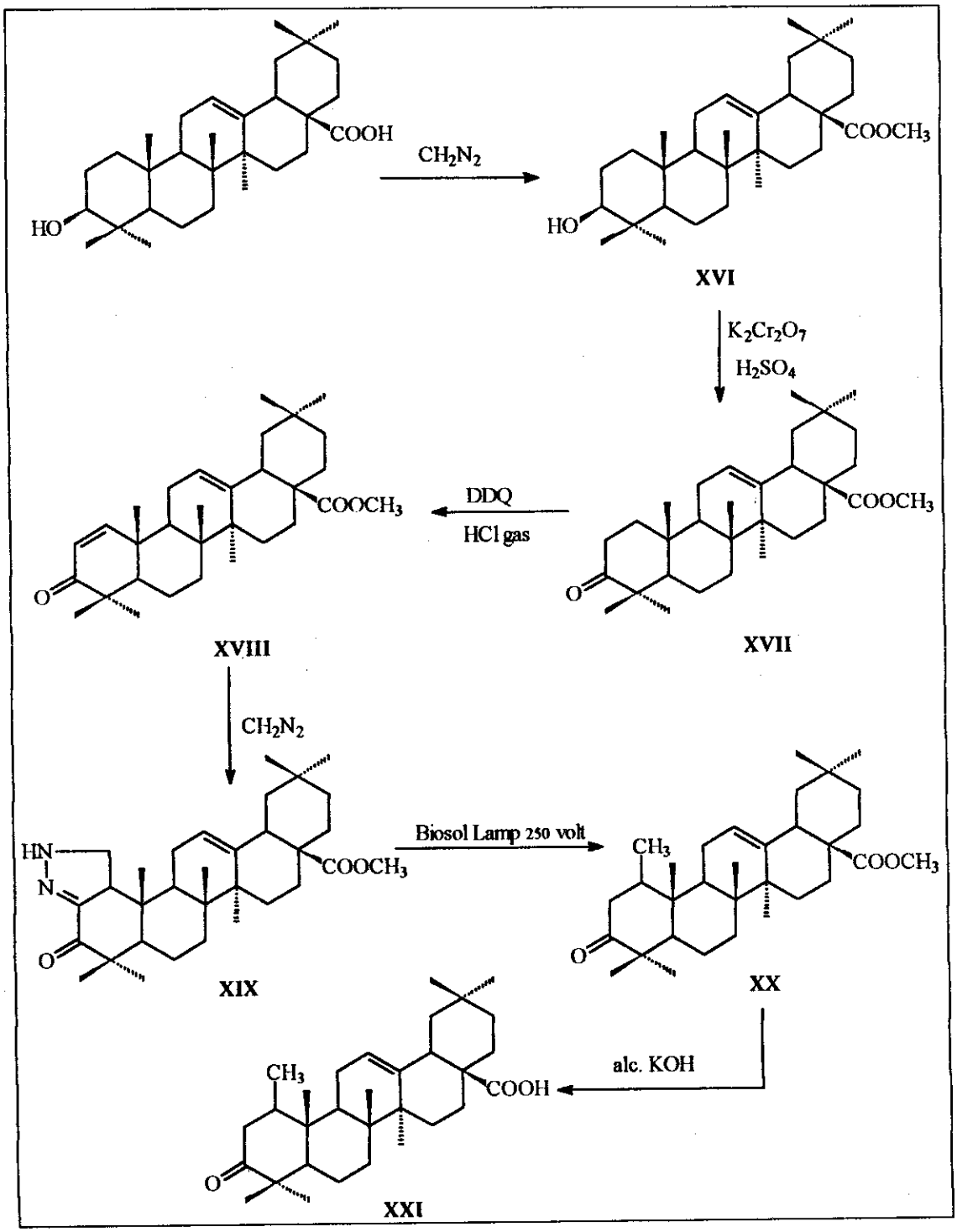
COOH
HO
CH_2N_2
$COOCH_3$
HO
XVI
$K_2Cr_2O_7$
H_2SO_4
$COOCH_3$
O
DDQ
HCl gas
$COOCH_3$
O
XVIII
XVII
CH_2N_2
HN
N
$COOCH_3$
O
XIX
Biosol Lamp 250 volt
CH_3
$COOCH_3$
O
XX
alc. KOH
CH_3
COOH
O
XXI

GC-MS of compound **XVIII** revealed the presence of M^+ at m/z 466 (1%) corrsponding its molecular structure $C_{31}H_{46}O_3$.

H-NMR-trace compound **XVIII** (Fig. 25) revealed the presence of the AB quarte pattern of the Δ^1-en-3-one at 4.2 ppm.

Treating of **XVIII** with diazomethane affored the corresponding pyrazoline derivative (**XIX**), where diazomethane adds it self on the Δ^1 (at locents 1 & 2) forming 1α,2α-pyrazoline fused ring A system.

The IR spectrum of compound **XIX** revealed the presence of C=N at 1623 cm^{-1}; while GC-MS of compound (**XIX**) revealed M^+ at 508 (28%) [$C_{32}H_{50}O_3$].

Irradiation[108a] of **XIX** in a water-cooled quartez reactor with high pressure Biosol Philips 250 watt quartz lamp for two hours cleavage the pyrazoline ring and yielded the methyl group at C-1 (compound **XX**). GC-MS of compound **XX** revealed the presence of M^+ at m/z 482 (8%) [$C_{32}H_{50}O_3$], the methyl protons at C-1 appear at 1.47ppm in the **H-NMR** trace of compound **XX**.

Alkaline hydrolysis of the methyl ester of compound **XX** afforded the corresponding 1-methyl 3-keto methyl oleanolic acid **XXI**. Its structure confirmed via the presence of OH absorption band at 3424 cm^{-1} in its IR spectrum. GC-MS of compound **XXI** revealed the presence of M^+ at m/z 468 (8%) [$C_{31}H_{48}O_3$].

Both compounds **XX** and **XXI** are the starting materials that meet for the three previous items aimed to be studied in the course of reaction with different patterns of substituted aromatic aldehydes.

Reaction with Aldehydes

Carring out the Aldol condensation of **XX** with different patterns of the substituted aromatic aldehydes with different inductive or mesomeric effects value (namely benzaldehyde, 4-chlorobenzaldehyde, 4-nitro-benzaldehyde and 2,4-dinitrobenzaldehyde) afforded the corresponding arylidene derivatives **XXIIa-d**, the α-ethoxy benzyl analogues **XXIIIa-d** and α-hydroxybenzyl analogues **XXIVa-d**. They were separated useing medium pressure chromatography.

^{1}H-NMR of compound **XXIIa** revealed the presence of both aromatic and arylidene protons resonating near 7.27-7.50 and 7.8 ppm, while the IR spectrum of **XXIIc** showed the arylidene conjugated system absorption band at 1651 cm^{-1}.

EI-MS of compound **XXIIb** revealed the presence of M^+ and M^++2 at m/z 604.5, 606.5 (3:1) [$C_{39}H_{53}O_3Cl$].

The structure elucidation of derivatives **XXIIIa-d** was supported by the presence of the methyl and methylenoxy protons of the α-ethoxy benzyl resonating at 1.40 and 3.91 ppm, while the aromatic protons resonating at 7.31-7.51 ppm in the **H-NMR** spectrum of compound **XXIIId**. Also, no arylidene absorption band was detected in the IR spectrum of compound **XXIIIb**.

Liquid ion mass spectrum of compound **XXIIIa** revealed M^++1 at m/z 617 (8%) [$C_{41}H_{61}O_4$].

The structure elucidation of derivatives **XXIVd** was based on examination of the IR, MS, ^{1}H-NMR and ^{13}C-NMR.

IR spectrum of compound **XXIVd** revealed the appearance of OH absorption band at 3541 cm^{-1} and no arylidene absorption band was detected.

^{1}H-NMR of compound **XXIVc** revealed wither ethoxy nor arylidene protons, but only the aromatic protons resonated at 7.5 ppm.

LI-MS of compound **XXIVd** revealed the presence of M^+ at m/z 678 (5%).

^{13}C-NMR of compound **XXIVa** (Fig. 26) revealed 30 peakes for the 30 carbon atoms skeleton beside six aromatic carbon atoms resonating near 128.1, 128.4, 128.0 ppm, while the methylene bridge carbon carrying α-OH resonated at 55.0 ppm.

Another chemical proof for the structure of compounds **XXII**, **XXIII** and **XXIV** came from conversion of derivative **XXII** into the corresponding α-ethoxy analogues **XXIII** via treating with sodium ethoxide in refluxing ethanol, products **XXIII** were produced due to the Retrograde 1,4-Michel addition of the ethoxide anion on the arylidene.

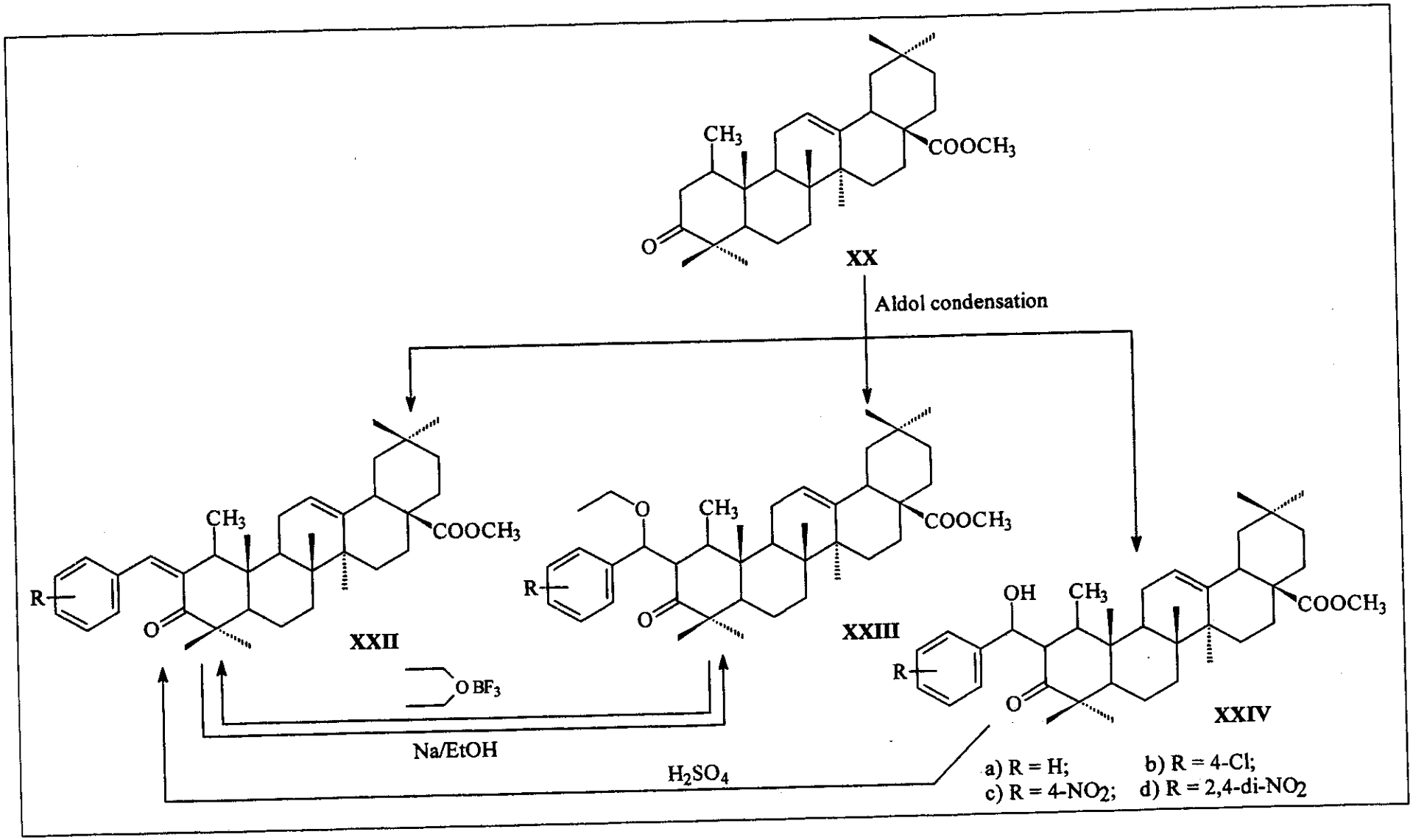
CH3
COOCH3
O
XX
Aldol condensation
R
CH3
COOCH3
O
XXII
O
CH3
COOCH3
R
O
XXIII
OH
CH3
COOCH3
R
O
XXIV
O BF3
Na/EtOH
H2SO4
a) R = H;
b) R = 4-Cl;
c) R = 4-NO2;
d) R = 2,4-di-NO2

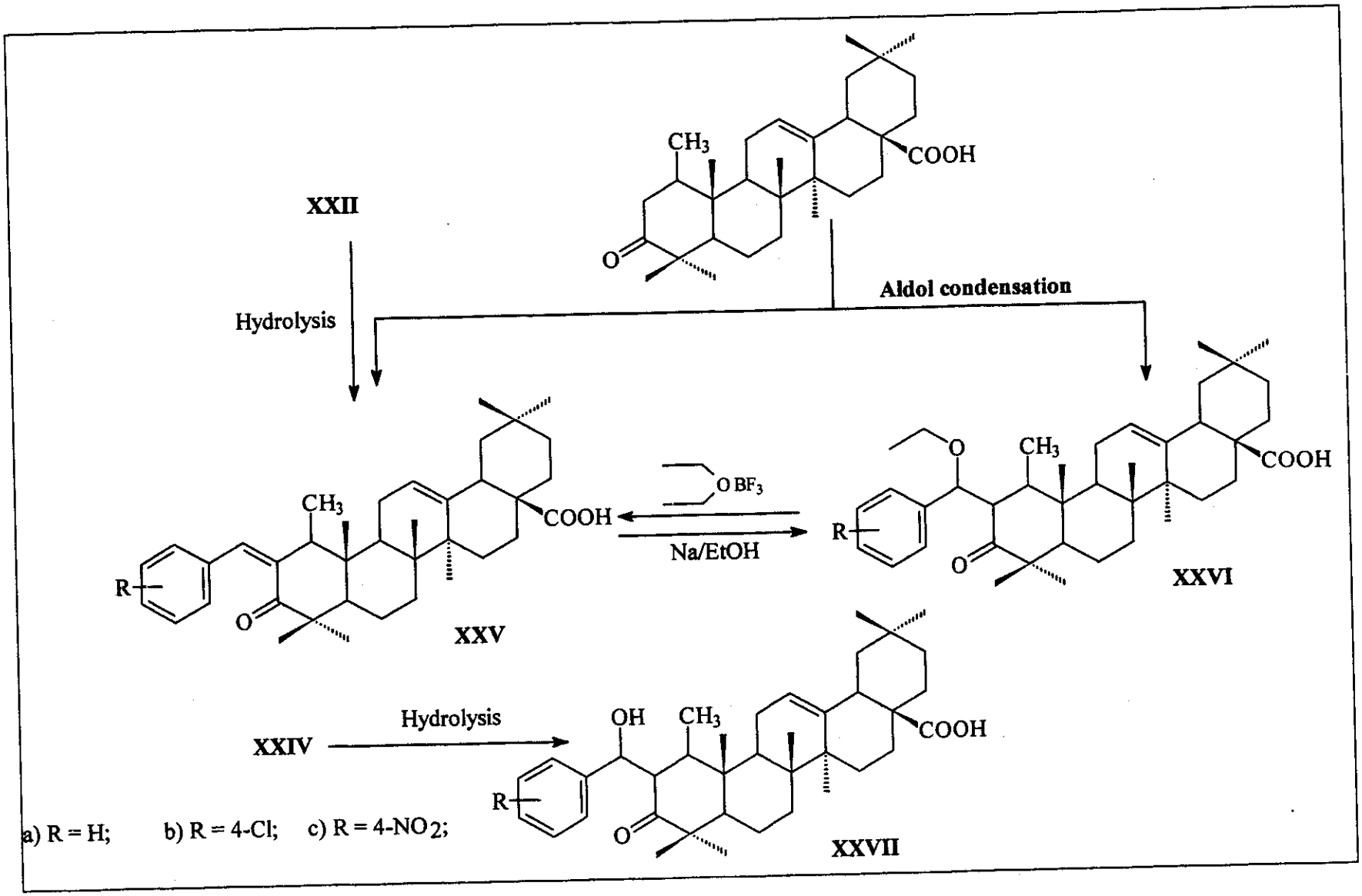
XXII
Hydrolysis
Aldol condensation
CH3
COOH
O
O BF3
Na/EtOH
R
XXV
XXVI
XXIV
Hydrolysis
OH
XXVII
a) R = H; b) R = 4-Cl; c) R = 4-NO2;

Mechanism of Aldol Condensation in Triterpenoids

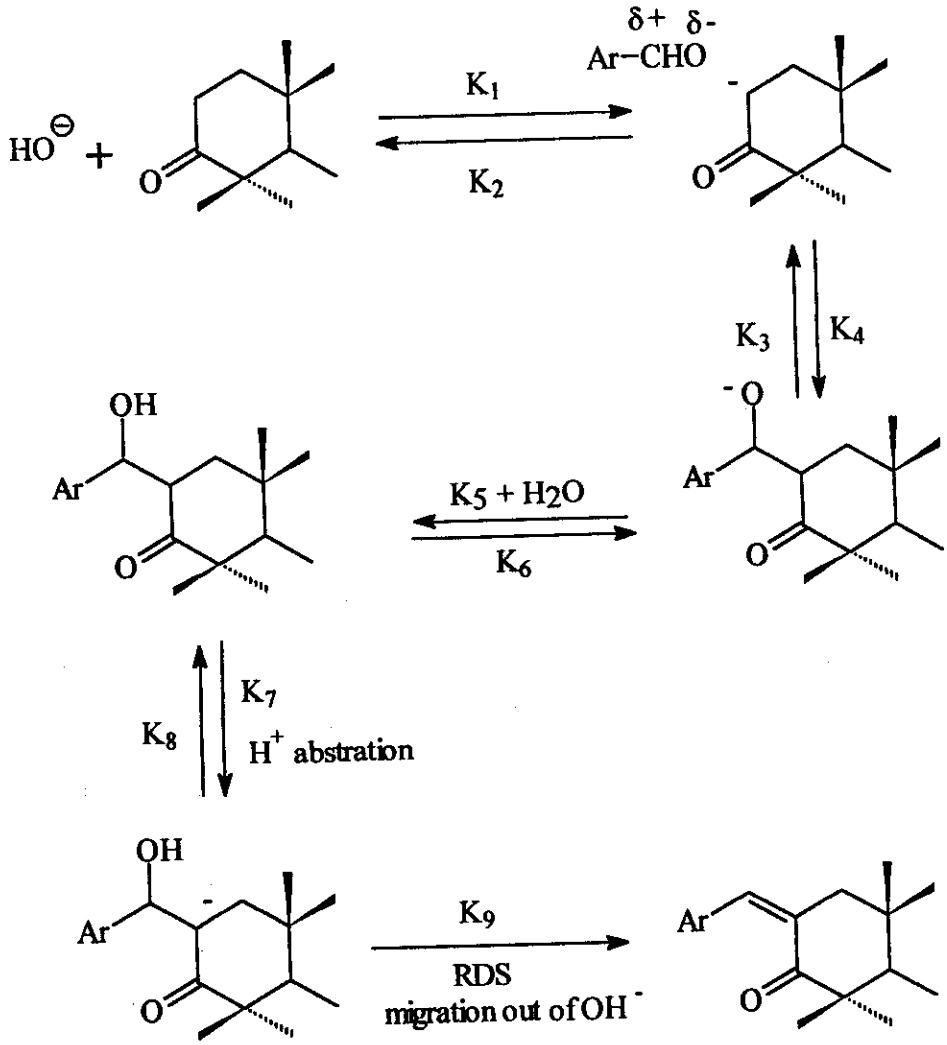

N.B.

The α-hydroxy benzyl derivatives were formed due to no migration out of the hydroxy group from non resonance stabilized anion due to 1,4-axial buttresing.

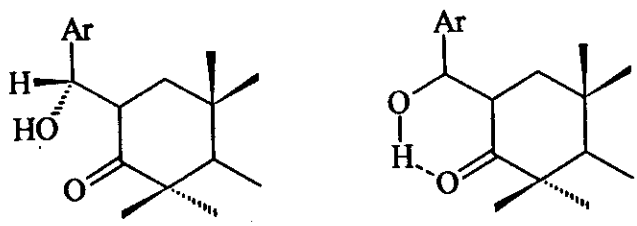

1,4-axial buttresing

Mechanistic Pathway of 1,4 Retrograde Michael Addition:

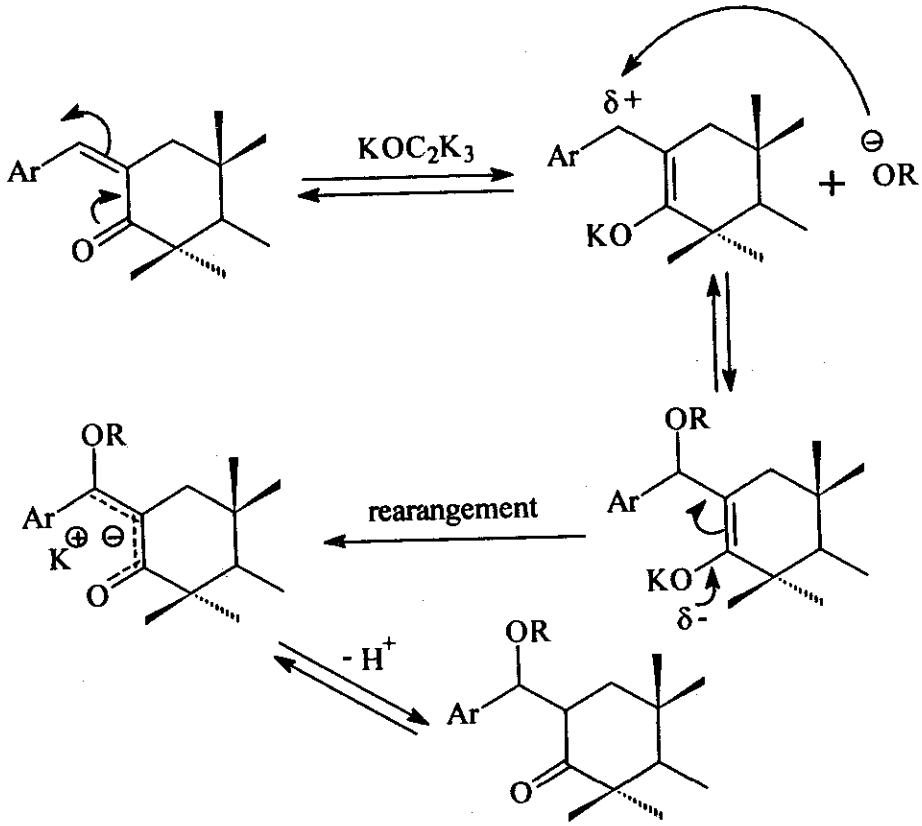

Mechanistic Pathway of the reaction of ethereated boron trifluride with α-ethoxybenzyl derivatives.

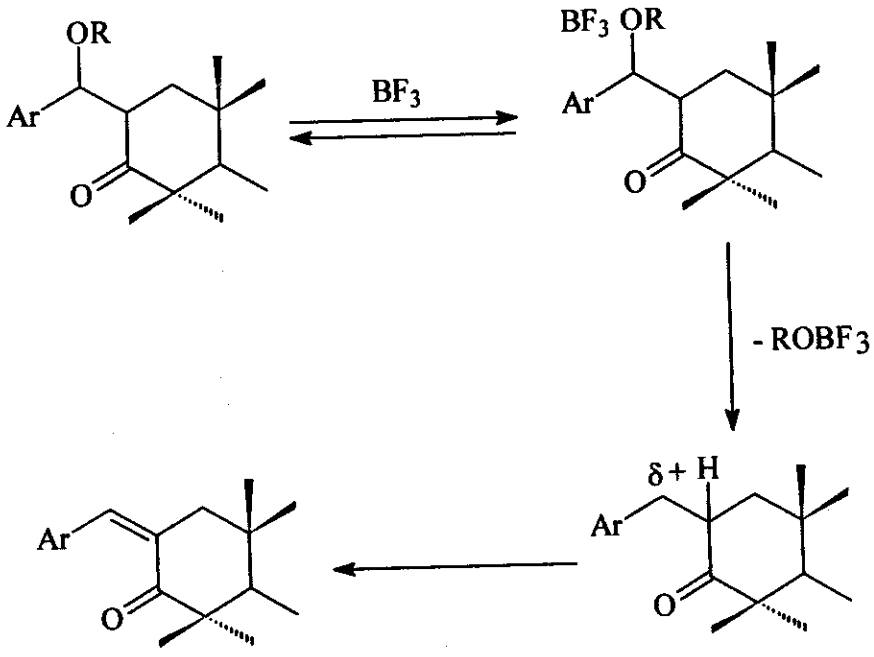

Conversion of derivatives **XXIII** to **XXII was** carried out by the aid of etherated boron trifluoride that abstracts ethanol from the α-benzyl part leading to the formation of the double bond of the arylidene derivative **XXII**.

The dehydration of derivatives **XXIV** with conc. H_2SO_4 lead to the formation of the arylidene derivatives **XXII** in good yield (mixed m.p., mixed TLC, finger print IR used to confirm the structure of the obtained derivatives in each cases).

It is worthy to mentioned that many trails were done to add a molecule of water on the arylidene derivatives **XXII** to obtain the corresponding α-hydroxy analogues **XXIV** but had meat no success.

Repeating the same above mentioned aldol condensation but replacing compound **XX** with its acid analougue **XXI** and excluding the 2,4-dinitrobenzaldehyde due to low yields and slow rate of reaction (need 14 days) gave only two reaction products. The first were the arylidene analougues **XXVa-c** and the α-ethoxy benzyl analogues **XXVIa-c** but no α-hydroxybenzyl analogues were isolated propaply due to the ease of separating a molecule of water from the transition state via the cage effect of the COO^-.

The structure of derivatives **XXV** was confirmed via IR, ^{1}HNMR and MS spectral data. ^{1}H-NMR of compound (**XXVa**) revealed the presence of aromatic and arylidene protons resonated at 7.19-7.50 and 7.9 ppm. IR spectrum of compound **XXVb** showed enone absorption

band at 1648 cm^{-1}. GC-MS spectrum of compound **XXVc** revealed M^+ at m/z 601 (B^+) [$C_{38}H_{51}NO_5$].

Confirming the structure of derivatives **XXVI** was achived from ^{1}H-NMR spectrum of compound **XXVIa** that showed α-methylenoxy and aromatic protons resonating at 3.71 and 7.6-7.70 ppm, while no arylidene proton was detected, IR spectrum of compound **XXVIb** shows no arylidene absorption bands.

EI-MS spectrum of compound **XXVIa** shows M^+ at m/z 602 (1.43%) [$C_{40}H_{58}O_4$]. FAB-MS of compound **XXVIc** (Fig. 27) shows M^+ at m/z 647 (4%) [$C_{40}H_{57}NO_6$].

Another chemical proof for the structure of both derivatives **XXV** and **XXVI** came from the conversion of derivative **XXV** into (**XXVI**) via treating with sodium ethoxide and the conversion of derivative **XXVI** into **XXV** via treating with etherated boron trifloride as mentioned before. It is worthy to mention that alcoholic KOH hydrolysis of derivatives **XXIIa-c** afforded the corresponding derivatives **XXVa-c** .

So, the α-hydroxybenzyl analogues **XXVIIa-c** are achieved via alcoholic KOH hydrolysis of derivatives **XXVa-c** which meat a great success. On carrying the alcoholic KOH hydrolysis of derivatives **XXIII**, the reaction product showed multispot TLC and was difficult to be separated.

EI-MS spectrum of both compounds **XXVIIa** and **XXVIIb** revealed their M^+ at m/z 574 and 619 (1.8 %). ^{1}H-NMR and IR spectra of compound **XXVIIc** is in accordance with the assigned structure.

4.3.1.2. Reactions of oleanolic acid lactone

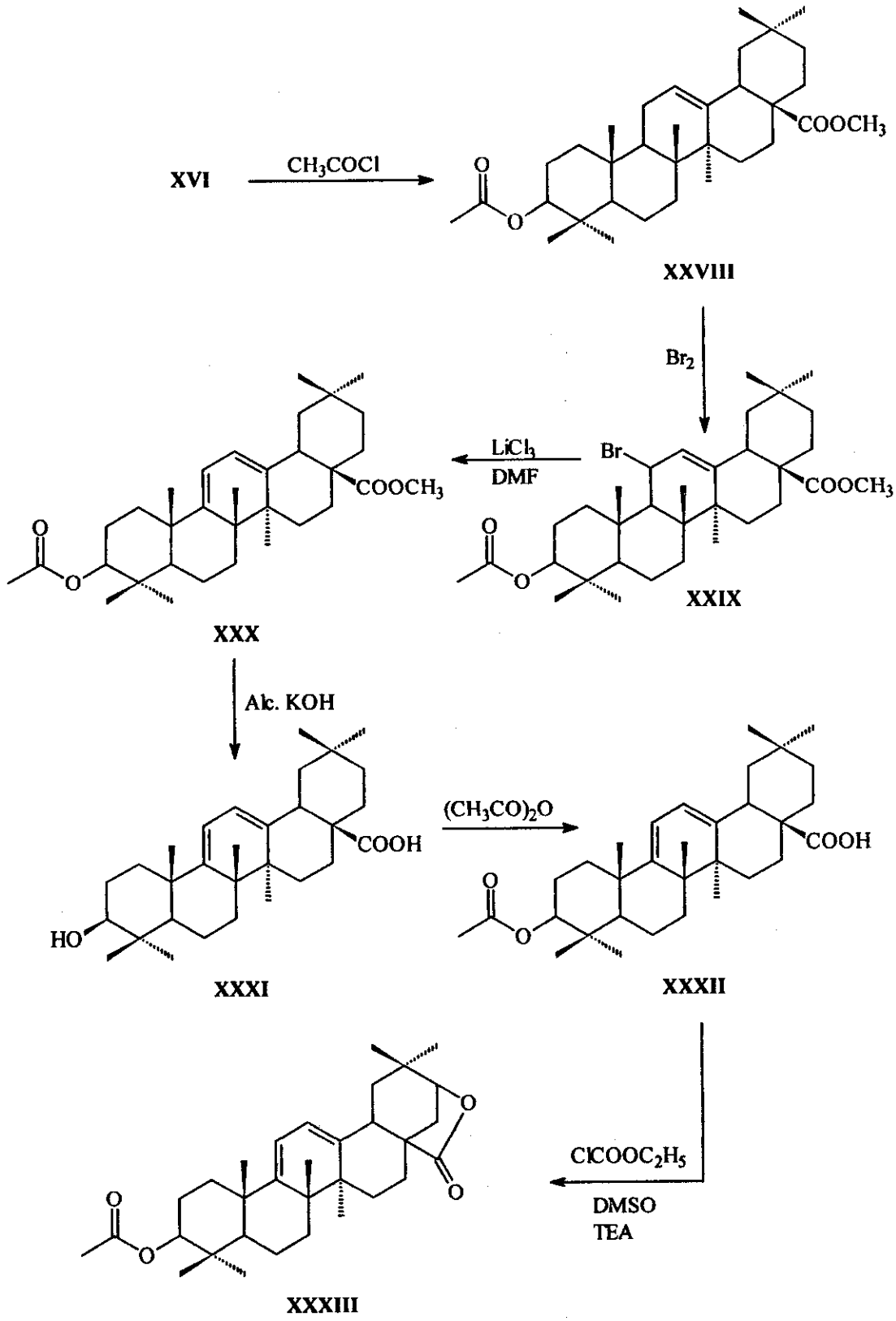

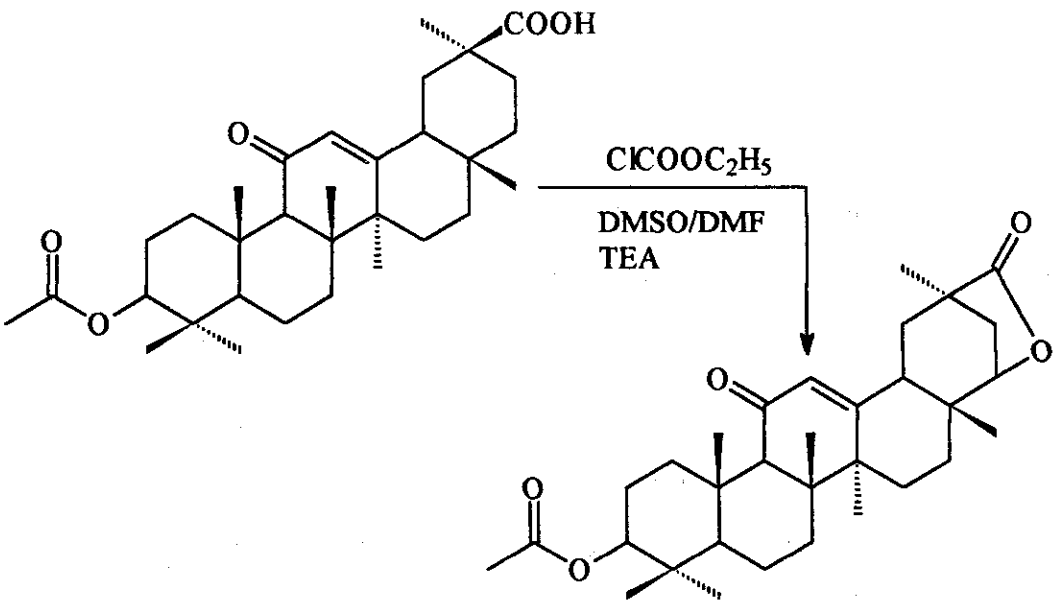

It was stated previously[109] that, the reaction of 3-acetyl glyceyrrhetic acid with ethyl chloroformate in DMSO and DMF gave the lactone 30→22

So, it was aimed to repeat the same reaction on oleanolic acid derivative containing extra double bond in ring C to obtain derivatives with OH group at locent 21 and extra double bond $\Delta^{9,12}$-diene. Such structure profile was expected to have potential increased anti-inflammatory activity.

The adopted synthetic pathway to achieve such tactic depends firstly on acetylation of oleanolic acid with acetyl chloride to prepare 3β-acetyl oleenolic acid **XXVIII**.

Allylic bromination of compound **XXVIII** at locent 11 in ring C with 2,3-dibromo methyl hydantoin afforded the corresponding 11 bromo derivative **XXIX** which was dehydrobrominated by boiling with $LiCl_3$/DMF to give corresponding $\Delta^{9,12}$-diene **XXX**.

IR spectrum of compound **XXVIII** revealed the disappearance of hydroxyl group absorption band. ^{1}H-NMR spectrum of compound **XXX** (Fig. 28) revealed olefenic protons at locent 11 & 12 resonatic at 5.8 ppm (AB quartet).

Alcoholic KOH hydrolysis of compound **XXX** gave **XXXI**. The latter derivative treated with acetic anhydride to yield the 3β-acetoxy derivative **XXXII**.

On treating the latter derivative **XXXII** with ethyl chloroformate in DMF/DMSO in the presence of triethylamine gave the C-30→20 lactone derivative **XXXIII**.

The structure of compound **XXXIII** was confirmed by IR, ^{1}H-NMR, GC-MS and Dept. spectroscopy.

IR spectrum of compound **XXXIII** revealed no hydroxyl group absorption band and the presence of lactone group absorption band at 1797 cm^{-1}, EI-MS spectrum of compound **XXXIII** revealed M+ at m/z 494 (3%) [$C_{32}H_{46}O_4$].

^{1}H-NMR spectrum of compound **XXXIII** showed the AB-quartet pattern of $\Delta^{9,12}$-diene at 5.7 ppm, beside the lactone ring C-21, equatorial proton resonating at 4.5 ppm (Fig. 29).

Dept spectroscopy of compounds **XXXIII** (Fig. 30) gave the final good proof for the structure elucidation of this compound.

4.3.1.2.1. Reaction with anilines

Treating derivative **XXXIII** with different pattern of substituted aniline derivatives afforded the corresponding C-28 anilide esters with C-21 hydroxyl group, due to opening of the lactone ring by the nucleophilic attack of lone pair of NH_2.

FAB-MS of compound **XXXIVb** (Fig. 31) revealed M^+ at m/z 647 (B^+) [$C_{40}H_{57}NO_6$].

EI-MS spectrum of compound **XXXIVd** revealed M^+ at m/z 601 (B^+) [$C_{39}H_{55}NO_4$], IR spectrum of compound **XXXIVa** revealed the presence of C-21 (OH) absorption band at 3610 cm^{-1}.

^{1}H-NMR spectrum of compound **XXXIVe** shows the AB-quartet pattern of $\Delta^{9,12}$-diene resonating at 5.8 ppm and the aromatic protons resonating at 7.2-7.4 ppm.

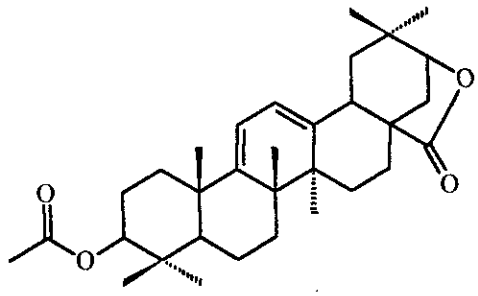

XXXIII

$ArNH_2$

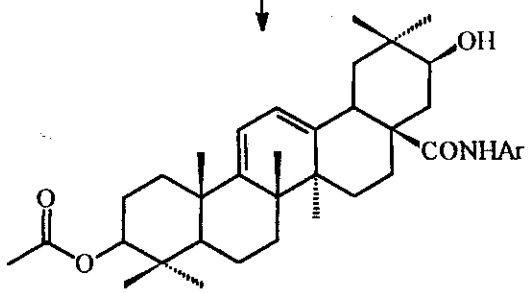

XXXIV

a) Ar = 4-chlorophenyl
b) Ar=2,4dimethoxyphenyl
c) Ar=2,5dimethoxyphenyl
d) Ar = 4-methylphenyl
e) Ar = 4-nitrophenyl

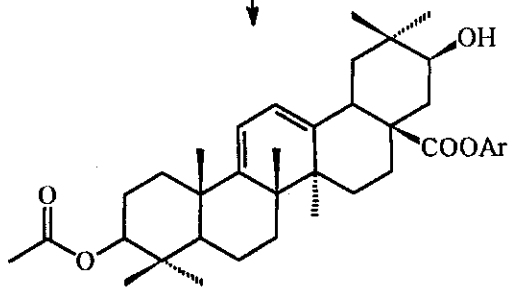

XXXV

a) Ar = 2-chlorophenyl
b) Ar = 4-chlorophenyl
c) Ar = 2-bromophenyl
d) Ar = 4-bromophenyl
e) Ar = 4-nitrophenyl

4.3.1.2.2. Reaction with phenols

On the other hand treating derivatives **XXXIII** with different pattern of substituted phenols derivatives **XXXV** with C21-eq (OH).

IR spectrum of compound **XXXVa** revealed the presence of OH at 3581 cm^{-1}. EI-MS spectra of both compounds **XXXVa** and **XXXVb** revealed the presence of their M^+ and M^++2 at m/z 622 and 624 (3:1). EI-MS spectra compound **XXXVe** revealed M^+ at m/z 633 (7%) (Fig. 32).

^{1}H-NMR spectrum of compound **XXXVd** showed the AB-quartet (5.8 ppm) pattern of $\Delta^{9,12}$-diene and the aromatic protons at 7.37-7.51 ppm.

Mechanistic pathway of lactone formation (Possible)

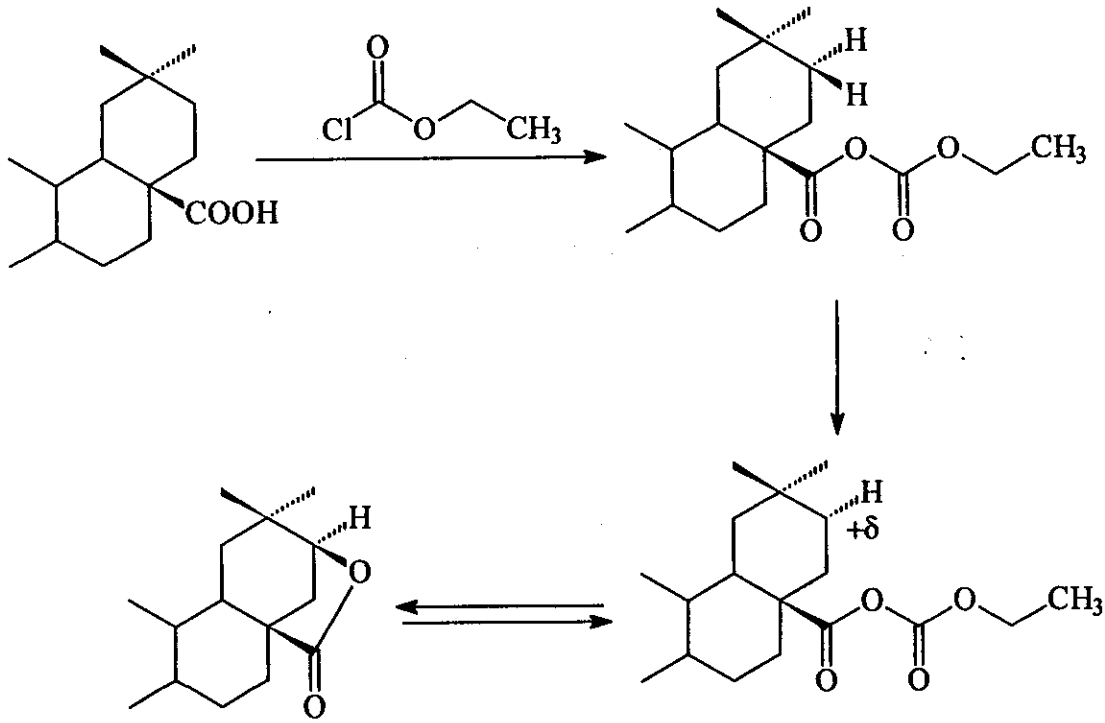

Possible mechanistic pathway of the nucleophilic attack on lactone

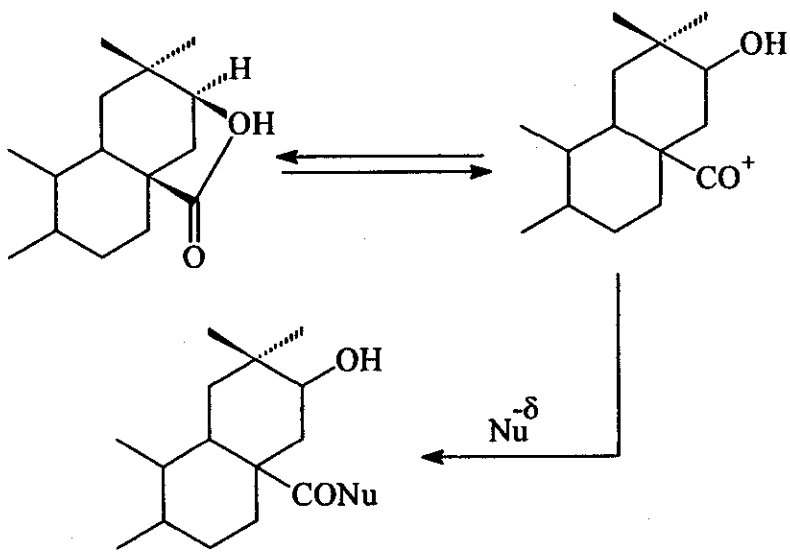

4.3.1.3. Construction of different types of heterocyclic ring systems (with one or two heteroatoms) and alicyclic ring systems fused in different manner to [3,2-x] ring A of the oleanolic acid skeleton.

Treating the 3-oxo-methyl aleanolate with either formaldehyde or acetaldehyde gave the corresponding formyledene and acetyledene derivatives XXXVIa,b, which serve as starting materials for building our target compound.

The synthetic design adopted for building up one heteroatom six membered ring system fused onto ring (A) of oleane skeleton. Involve reacting derivatives with active methylene containing compounds in which one electron withdrawing group is the cyano group, namely, ethyl cyano acetate[110-115], cyanoacetamide[116-121], malononitrile and thiocyano-acetamide[122-128].

The synthetic design adopted for building up alicyclic ring system fused to ring (A) of oleanolic acid involves the Robenson Annulated concept[129-132].

The synthetic design adopted for building up two heteroatom six membered ring system fused to ring (A) of oleanolic acid involve treating derivatives **XXXVIa,b** with diamino function containing compounds as guanidine and thiourea[133].

Treating of derivatives **XXXVIa,b** with ethyl cyanoacetate in ethanol in the presence of sodium ethoxide afforded the corresponding methyl-2`-oxo-3`-cyano-18β-olean[3,2-c]pyran-12-ene-28-oate **XXXVIIa** and methyl-2`-oxo-3`-cyano-6`-methyl-18β-olean[3,2-c]pyran-12-ene-28-oate **XXXVIIb**.

IR spectrum of compound **XXXVIIb** showed the appearance of CN absorption band at 2250 cm^{-1}, while EI-MS spectrum of compound **XXXVIIb** showed M^+ at m/z 559 (B^+) [$C_{36}H_{49}NO_4$]. The ^{1}H-NMR data of compound **XXXVIIa** is in accordance with the assign structure.

Treating of derivatives **XXXVIa,b** with ethyl cyanoacetate in n-butanol in the presence of eight folds of ammonium acetate gave the corresponding methyl-2`-oxo-3`-cyano-18β-olean[3,2-b]pyrido-12-en-28-oate **XXXVIIIa** and methyl-2`-oxo-3`-cyano-4`-methyl-18β-olean[3,2-b]pyrido-12-en-28-oate **XXXVIIIb**.

The spectral proof of these compounds based on the presence of cyano group absorption band at 2238 and C=O absorption band at 1638 cm^{-1}, also EI-MS spectrum of compound **XXXVIIIb** revealed M^+ at m/z 558 (B^+) [$C_{36}H_{50}N_2O_3$].

^{1}H-NMR spectrum of compound **XXXVIIIb** (Fig. 33) was in accordance with the proposed structure where the methyl protons of both carboxylate and that on pyridone resonating at 3.61 and 1.97 ppm.

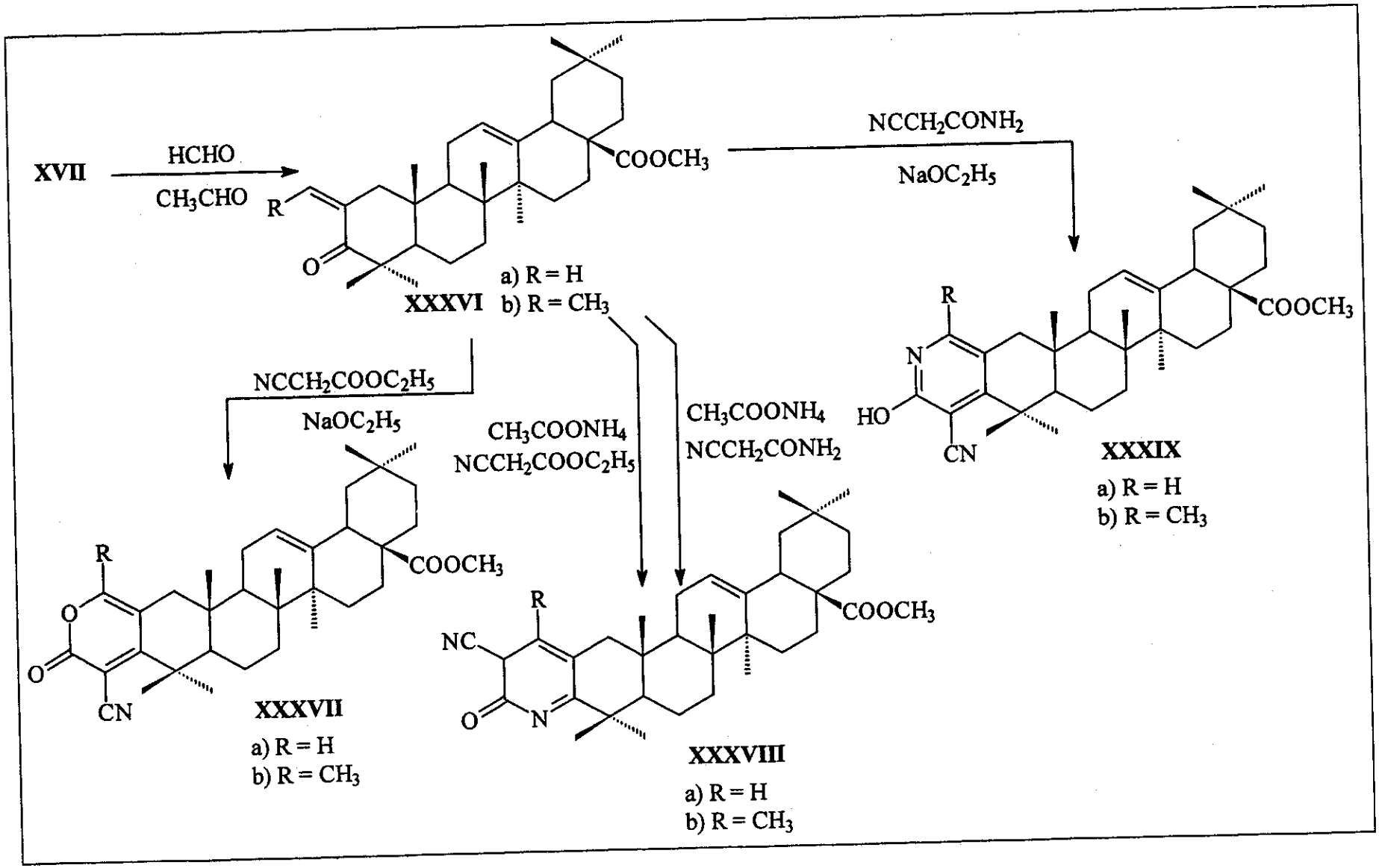
XVII
HCHO
CH3CHO
R
O
COOCH3
XXXVI
a) R = H
b) R = CH3
NCCH2CONH2
NaOC2H5
R
N
HO
CN
COOCH3
XXXIX
a) R = H
b) R = CH3
NCCH2COOC2H5
NaOC2H5
R
O
O
CN
COOCH3
XXXVII
a) R = H
b) R = CH3
CH3COONH4
NCCH2COOC2H5
CH3COONH4
NCCH2CONH2
R
NC
O
N
COOCH3
XXXVIII
a) R = H
b) R = CH3

Possible mechanistic pathway of the reaction of ethyl cyanoacetate with derivatives **XXXVI**

a) In the presence of NaOR

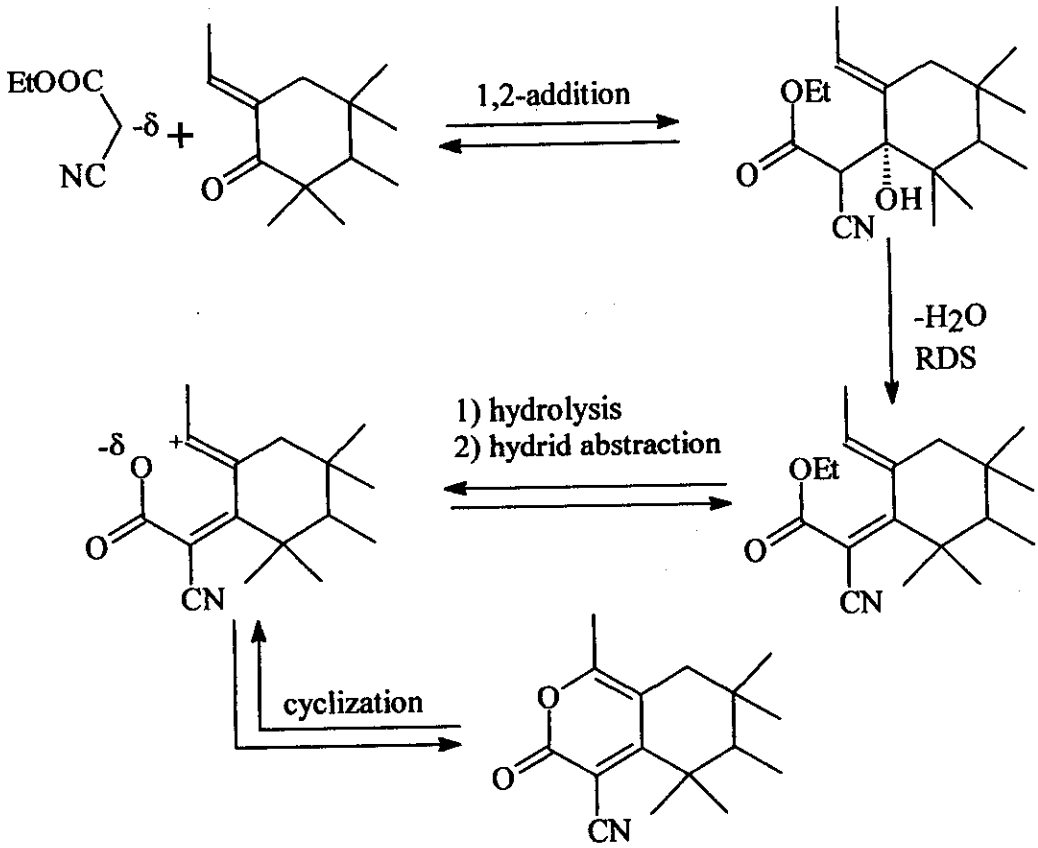

b) In the presence of ammonium acetate

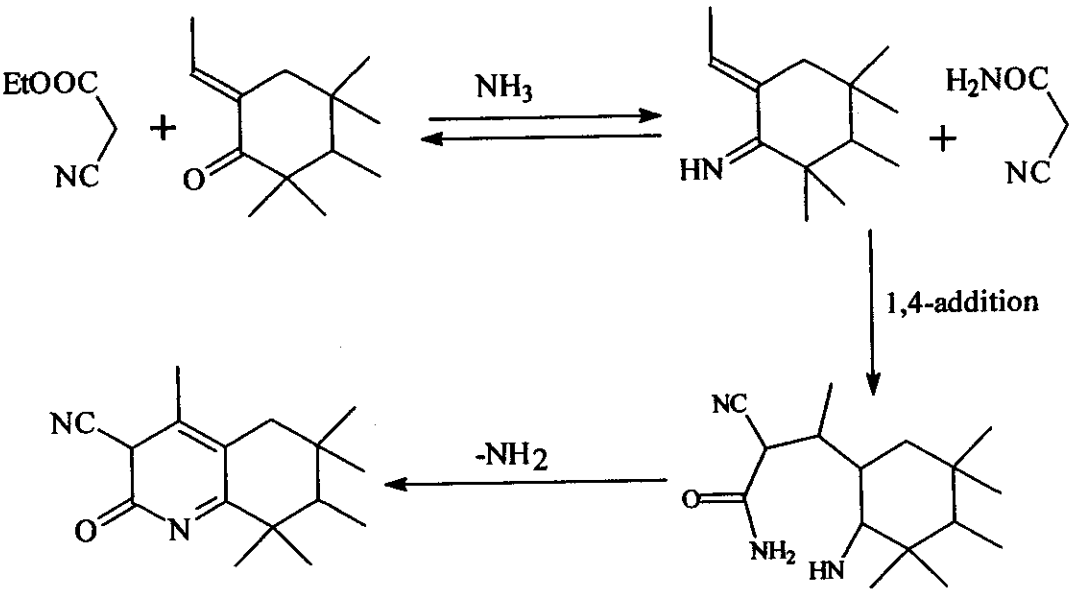

Possible mechanistic pathway of the reaction of ethyl cyanoacetamide with derivatives XXXVI

a) In the presence of NaOR

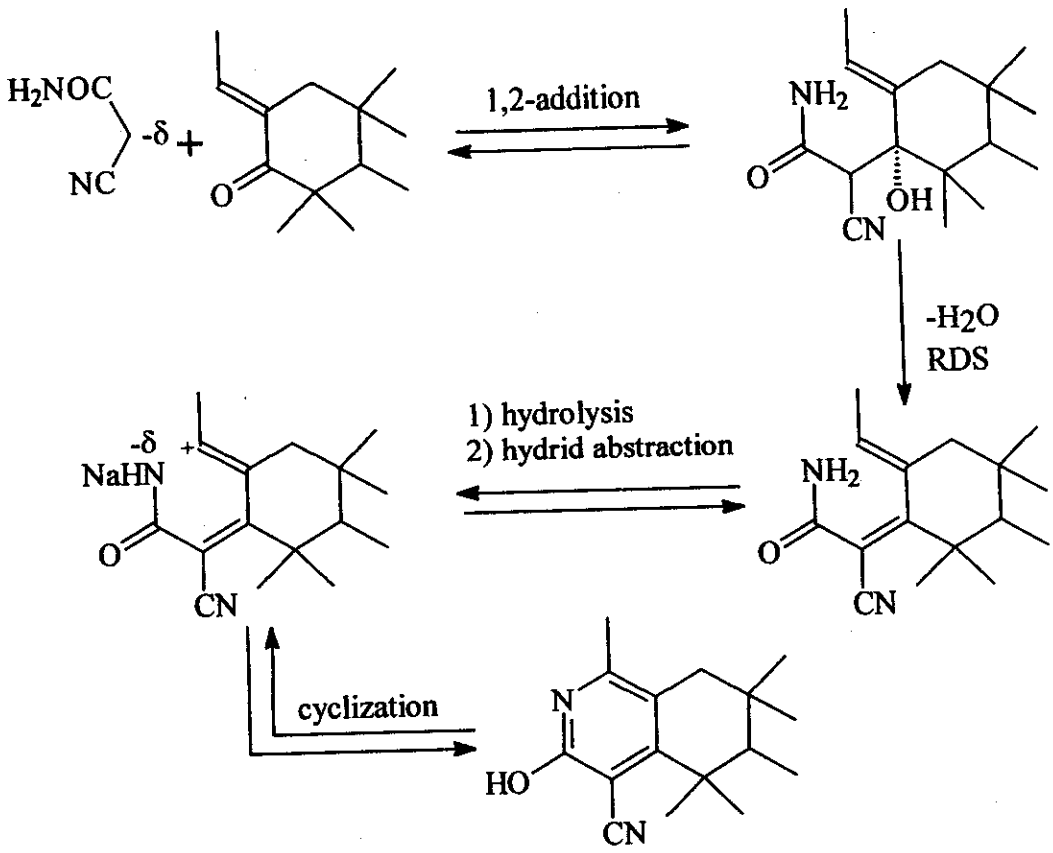

b) In the presence of ammonium acetate

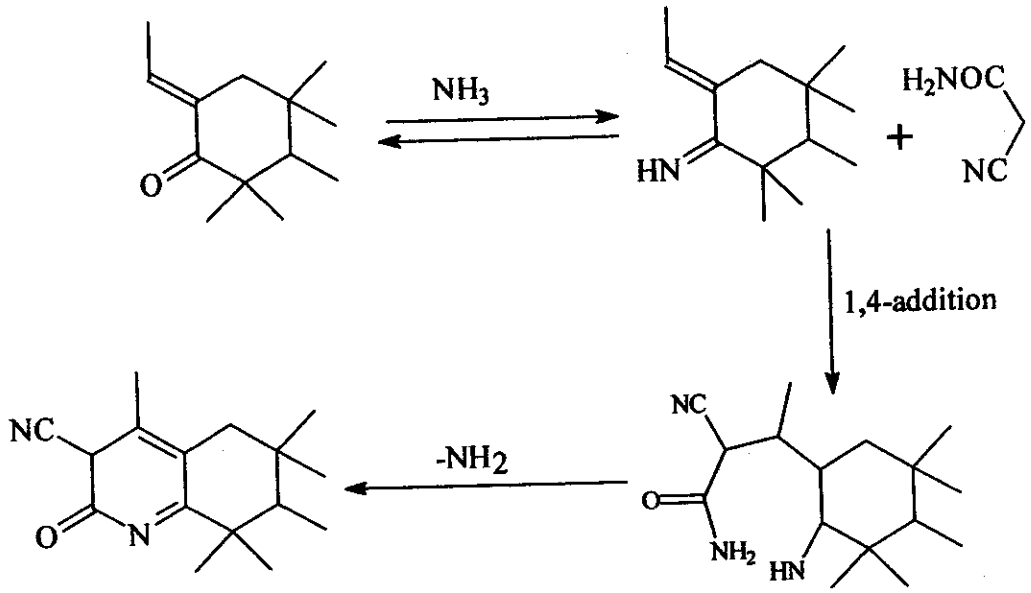

The chemical proof for derivatives **XXXVIIIa,b** came from that these derivatives could be prepared by another synthetic route via treating derivatives **XXXVIa,b** with cyanoacetamide in n-butanol in the presence of eight folds of ammonium acetate.

Repeating the latter reaction between derivatives **XXXVIa,b** and cyanoacetamide in ethanol in the presence of sodium ethoxide gave the corresponding 2`-hydroxy-3`-cyano-18β-olean[3,2-c]pyridine-12-en-28-oate **XXXIXa** and methyl-2`-hydroxy-3`-cyano-6`-methyl-18β-olean-[3,2-c]pyridine-12-en-28-oate **XXXIXb**.

IR spectrum of compound **XXXIXb** shows the appearance of CN absorption bands at 2250 cm^{-1} and the hydroxyl group absorption band at 3480 cm^{-1}. ^{1}H-NMR spectrum of compound **XXXIXa** (Fig. 34) revealed the presence of the following peaks at 3.57, 3.89 and 6.95 ppm corresponding to the methyl ester protons, hydroxyl proton and pyridyl proton respectively. EI-MS spectrum of compound **XXXIXb** revealed M^+ at m/z 558 (60%) [$C_{36}H_{50}N_2O_3$].

Reacting the derivatives **XXXVIa,b** with thiocyanoacetamide in ethanol in the presence sodium ethoxide afforded the corresponding methyl-2`-mercapto-3`-cyano-18β-olean- [3,2-c]pyridine-12-en-28-oate **XLa** and methyl-2`-mercapto-3`-cyano-6`-methyl-18β-olean- [3,2-c]-pyridine-12-en-28-oate **XLb**.

FT-IR spectrum of compound **XLb** revealed CN absorption band and SH absorption band at 2250 and 3423 cm^{-1}, respectively. ^{1}H-NMR spectrum of compound **XLa** revealed the presence of the following pearesat 2.9, 3.58 and 7.05 ppm corresponding to SH, $COOCH_3$ and pyridyl proton respectively. EI-MS spectrum of compound **XLb** showed M^+ at m/z 574 $[C_{36}H_{50}N_2O_2S]$.

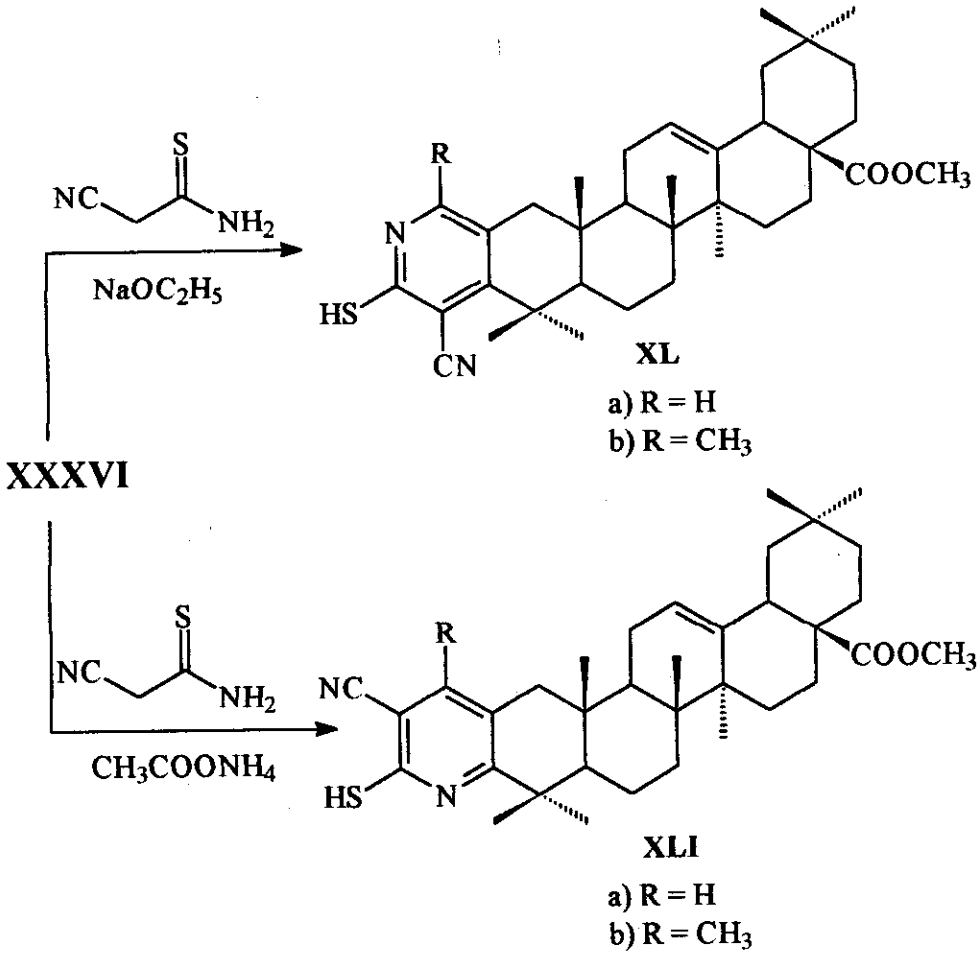

Repeating the same latter reaction between derivatives **XXXVI** with thio cyanoacetamide in the presence of eight folds of ammonium acetate instead of sodium ethoxide gave the corresponding methyl-2`-mercapto-3`-cyano-18β-olean[3,2-b]pyridine-12-en-28-oate and methyl-2`-mercapto-3`-cyano-4`-methyl-18β-olean[3,2-b]pyridine-12-en-28-oate **XLIa,b**.

The reaction of thiocyanoacetamide with derivatives XXXVIprobably takes place according to the following mechanism.

a) In the presence of NaOR

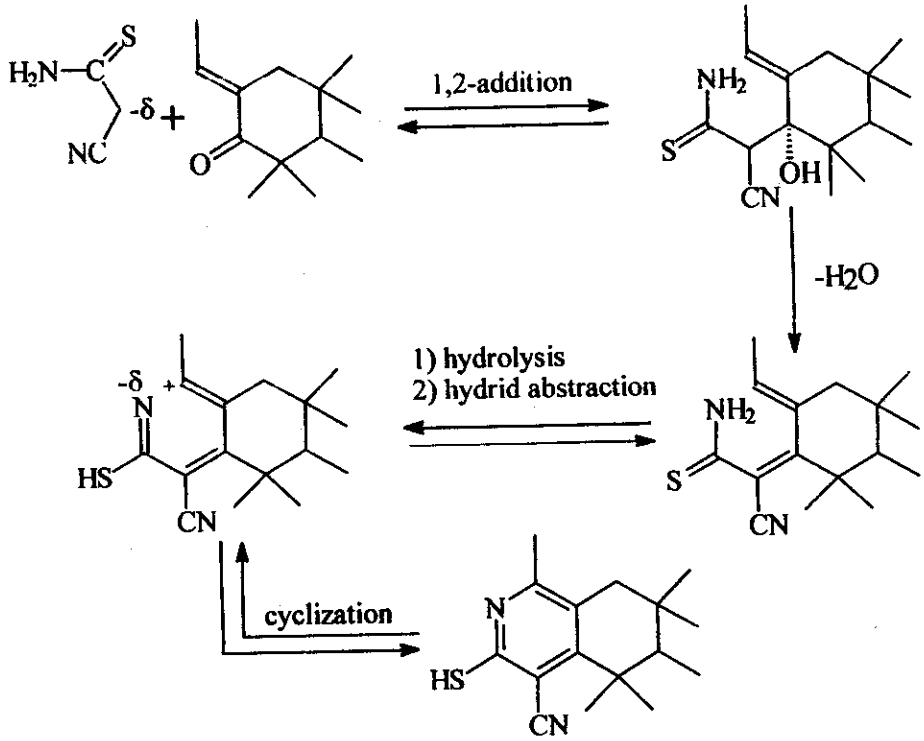

b) In the presence of ammonium acetate

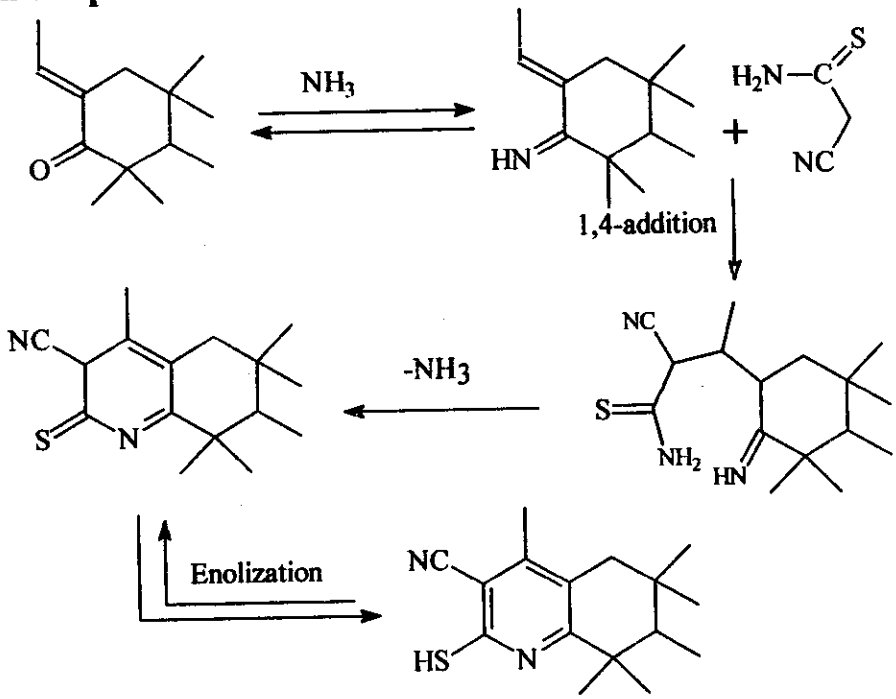

^{1}H-NMR spectrum of compound **XLIa** showed the presence of the following peaks at 2.8(s 1H SH),, 3.58 (s 3H $COOCH_3$)and 6.9(m pyridyl protons).

EI-MS spectrum of compound **XLIb** revealed M^+ at m/z 574 (67%) [$C_{36}H_{50}N_2O_2S$].

Carrying out the reaction between derivatives **XXXVIa,b** and malononitrile afforded the corresponding methyl-2`-ethoxy-3`-cyano-18β-olean[3,2-b]pyridine-12-en-28-oate **XLIIa** and methyl-2`-ethoxy-3`-cyano-6`-methyl-18β-olean[3,2-b]pyridine-12-en-28-oate **XLIIb**.

The presence of CN absorption band at 2251 cm^{-1} together with the O-CH_2 protons of the α-ethoxy resonating at 3.9 ppm are considered as a good evidence for the structure elucidation of this compounds.

Another evidence came from the EI-MS spectrum of compound **XLIIa** that revealed M^+ at m/z 572 (7%) [$C_{37}H_{52}N_2O_3$].

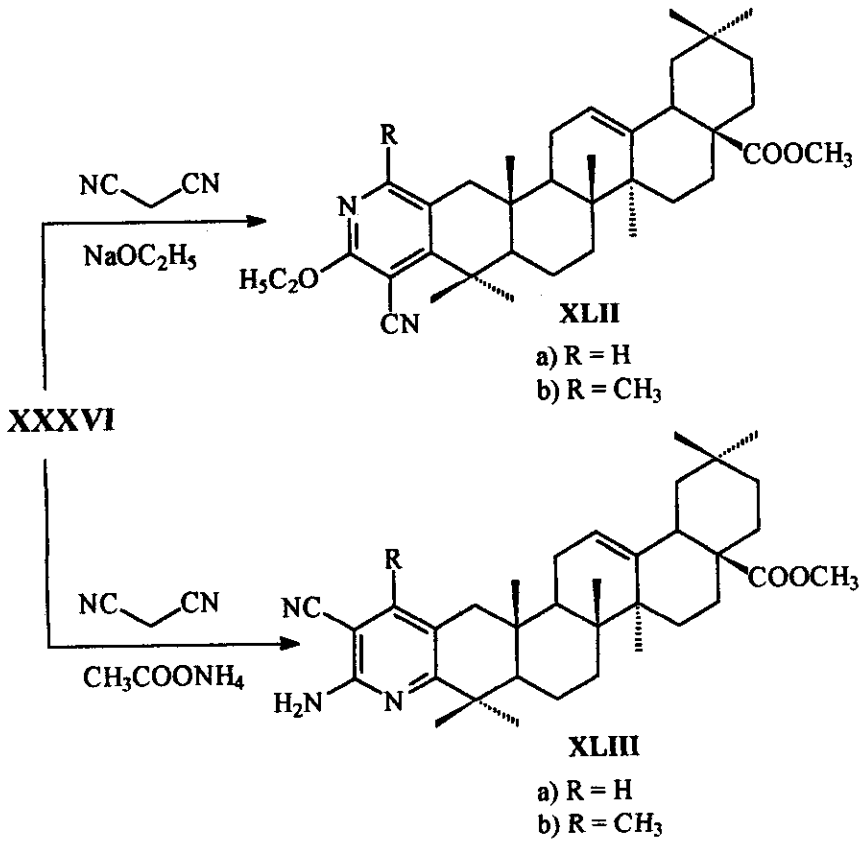

Repeating the latter reaction in the presence of eight folds of ammonium acetate instead of sodium ethoxide gave the corresponding methyl-2`-amino-3`-cyano-18β-olean[3,2-b]pyridine-12-en-28-oate **XLIIIa** and methyl-2`-amino-3`-cyano-4`-methyl-18β-olean[3,2-c]pyridine-12-en-28-oate **XLIIIb**.

IR spectrum of compound **XLIIIa** (Fig. 35) shows (NH_2) and (CN) absorption bands at 3423 and 2197 cm^{-1}, respectively.

^{1}H-NMR spectrum of compound **XLIIIb** (Fig. 36) shows the following peaks at 3.3, 3.48 attributed to CH_3 (on pyridine), $COOCH_3$. EI-MS spectrum compound **XLIIIa** revealed M^+ at m/z 543 (65%) [$C_{35}H_{49}N_3O_2$].

The reaction of malononitrile with derivatives XXXVI probably takes place according to the following mechanism.

a) In the presence of NaOR

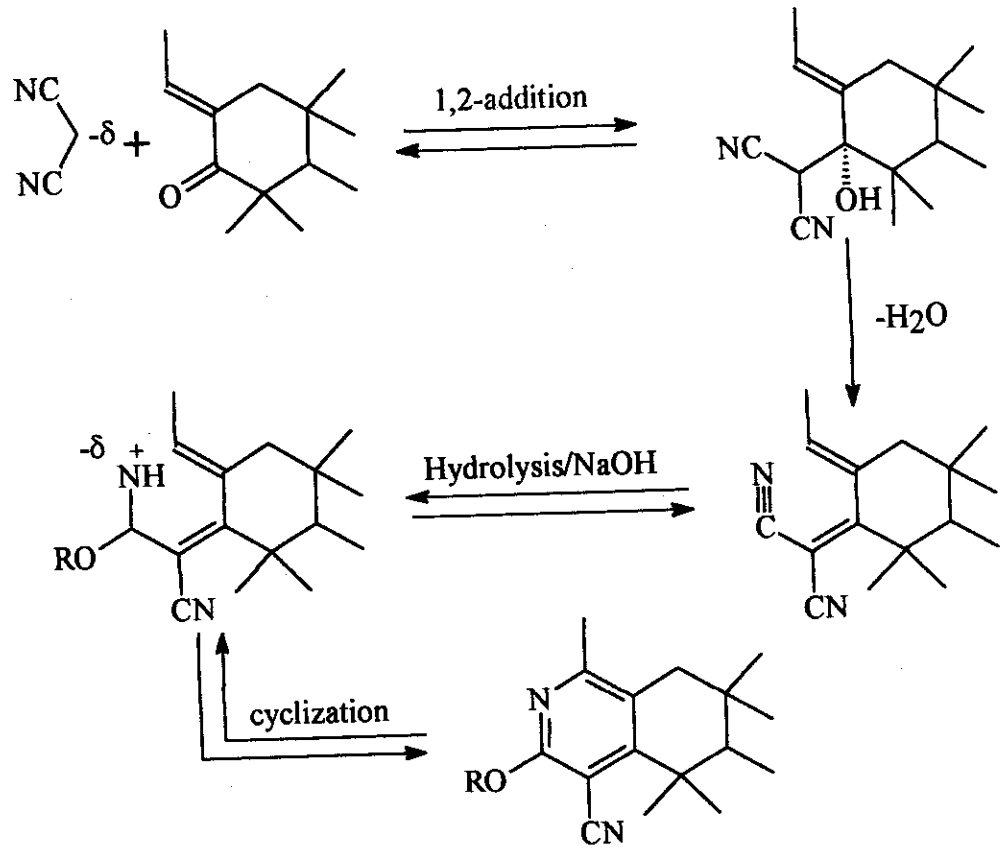

b) In the presence of ammonium acetate

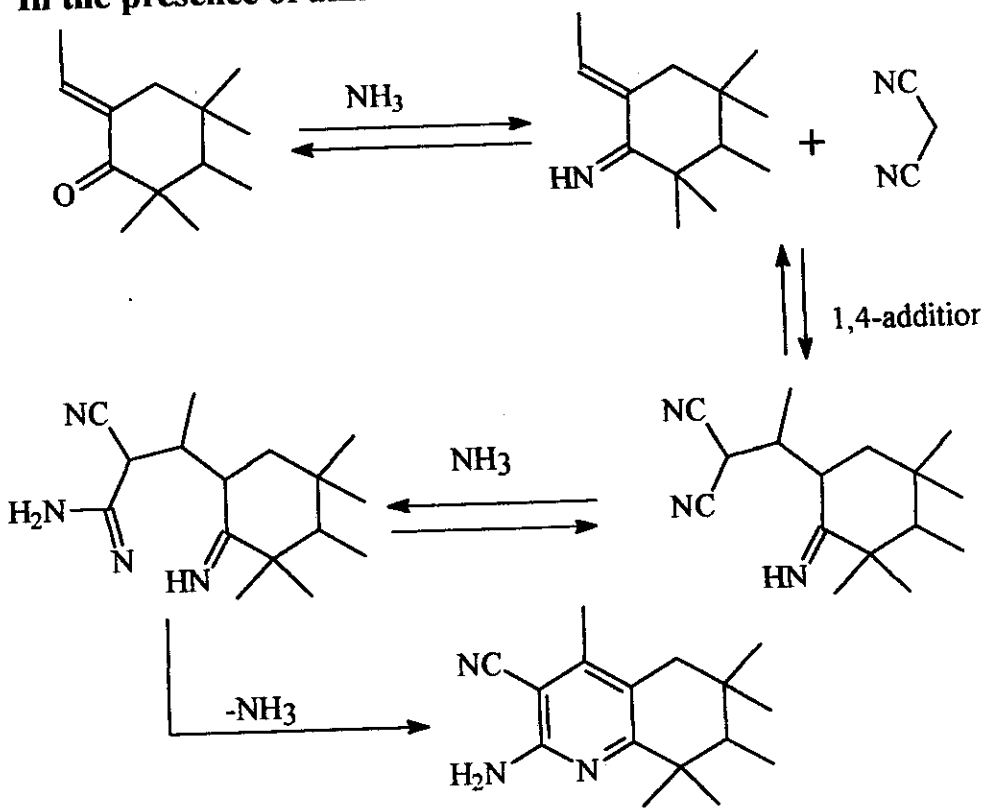

Robenson annulation[129-132] reaction of derivatives **XXXIVa,b** with ethyl acetoacetate in ethanol in the presence of sodium ethoxide affords the corresponding methyl 6`-ethylcarboxylate-1`-oxo-18β-olean[3,2-c]cyclohex-12,2`-diene-28-oate **XLIVa** and methyl-6`-ethylcarboxylate-1`-oxo-6`-methyl-18β-olean[3,2-c]cyclohex-12,2`-diene-28-oate **XLIVb**. While Robenson annulation with acetyl acetone gave the corresponding methyl-6`-acetyl-1`-oxo-18β-olean[3,2-c]cyclohex-12,2`-diene-28-oate **XLVa** and methyl-6`-acetyl-1`-oxo-6`-methyl-18β-olean[3,2-c]cyclohex-12,2`-diene-28-oate **XLVb**.

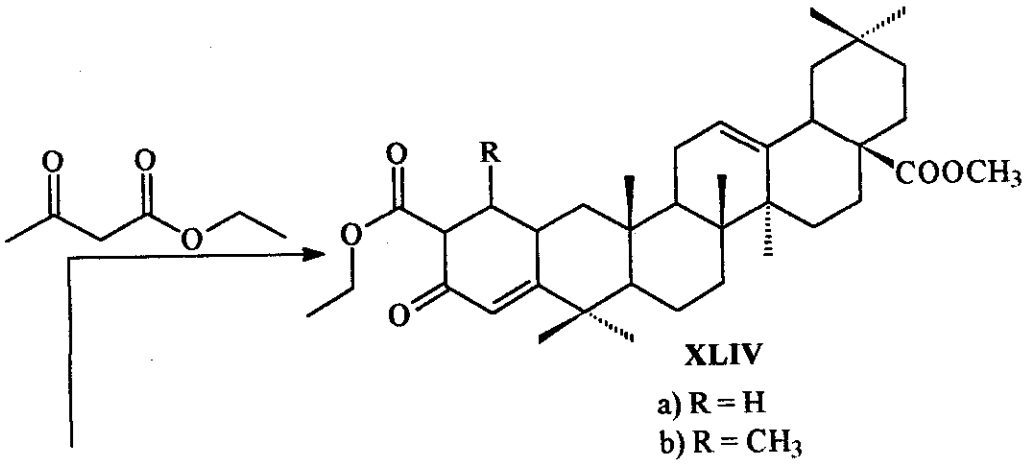

XLIV

a) R = H
b) R = CH_3

XXXVI

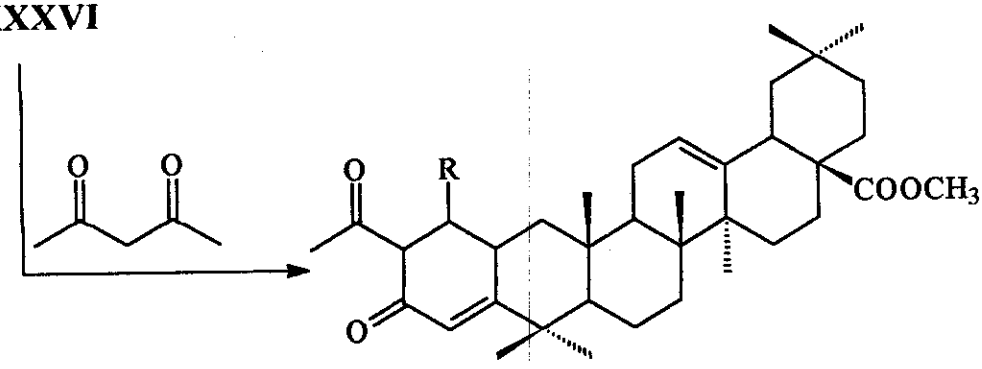

XLV

a) R = H
b) R = CH_3

The reaction of ethyl acetoacetate with derivatives **XXXVI** probably takes place according to the following mechanism.

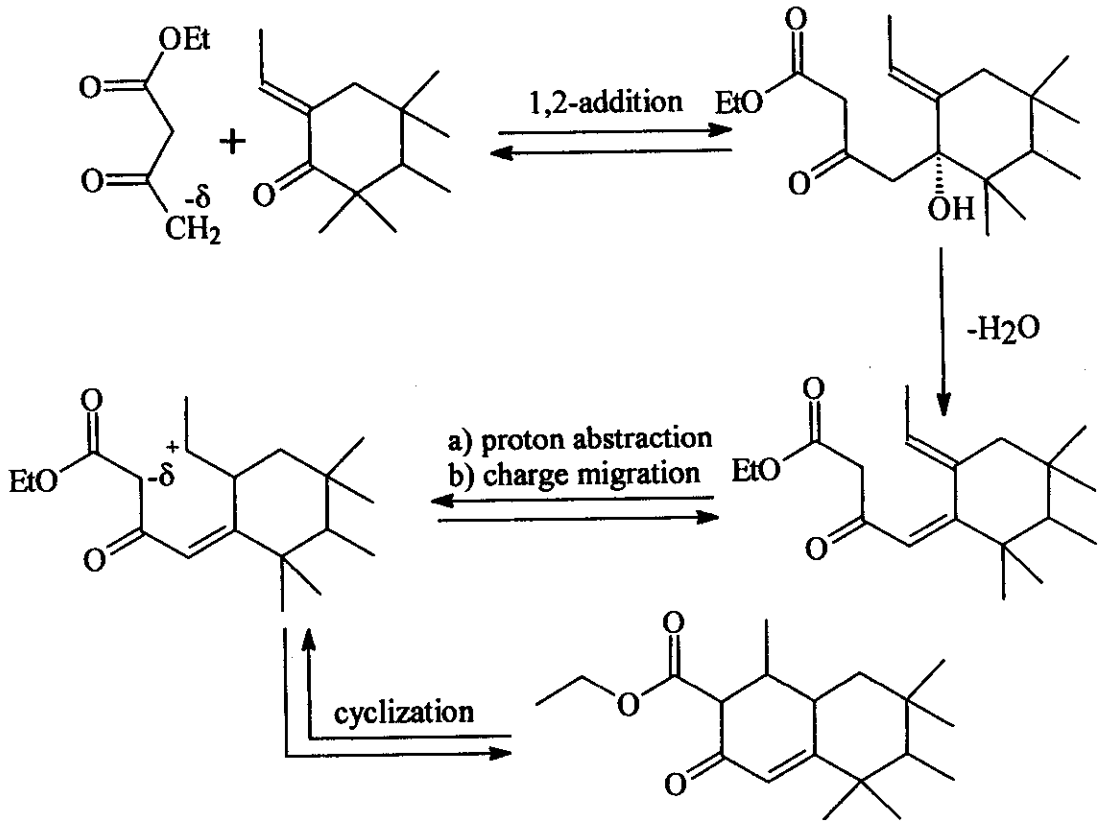

The reaction of acetyl acetone with derivatives **XXXVI** probably takes place according to the following mechanism.

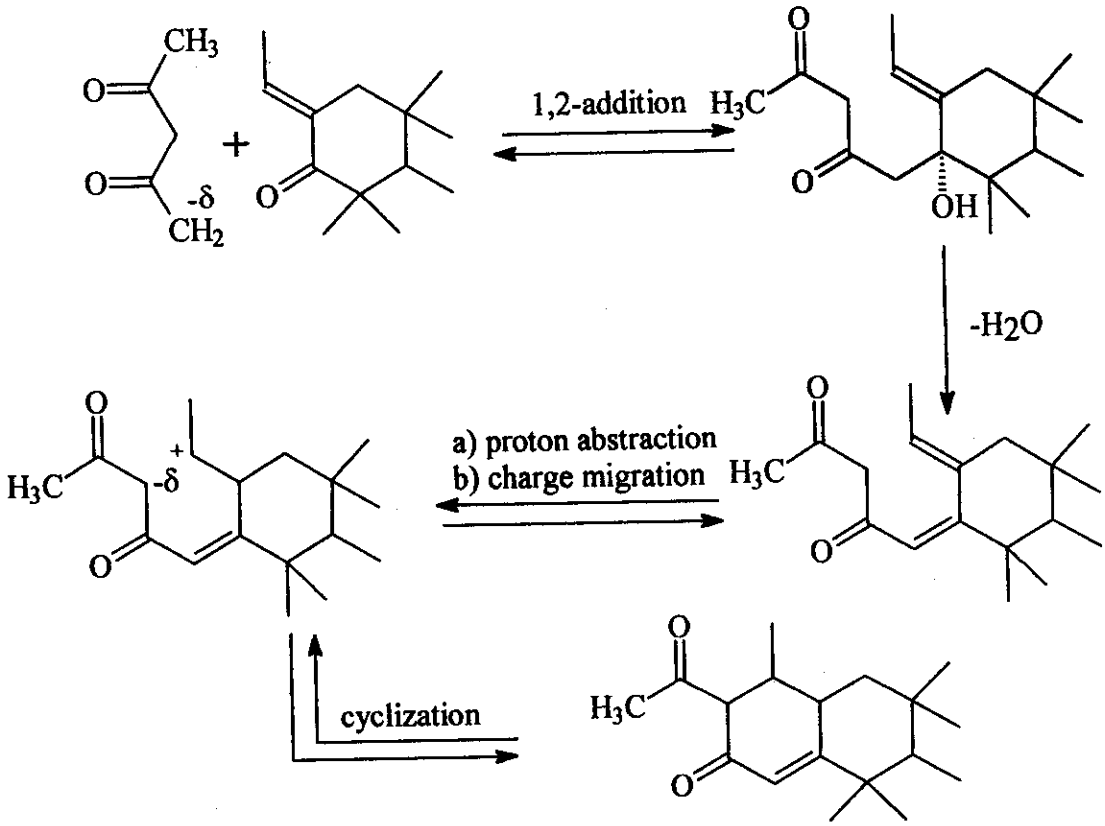

^{1}H-NMR spectrum of compound **XLIVa** revealed the presence of the following peaks at 3.81(m 3H $COOCH_3$, $COOCH_2$) 5.83 (enone protons of the cyclohexenone). While the ^{1}H-NMR spectrum of compound **XLVb** showed the following peaks at 1.91(s 3H $COCH_3$), 3.31(s 3H$COOCH_3$) and 5.7 (enone protons of the cyclohexenone).

FT-IR spectra of both compounds **XLIVb** and **XLVa** shows enone absorption bands at 1645 and 1637 cm^{-1} respectively. EI-MS spectrum of compound **XLIVb** revealed M^+ at m/z 606 (41%) [$C_{39}H_{58}O_5$]. EI-MS spectrum of compound **XLVb** revealed M^+ at m/z 576 (43%) [$C_{38}H_{56}O_4$].

Treating of the derivatives **XXXVI** with guanidine hydrochloride gave the corresponding methyl-2`-amino-18β-olean[3,2-d]pyrimidine-12-ene-28-oate **XLVIa** and methyl-2`-amino-6`-methyl-18β-olean[3,2-d]-pyrimidine-12-ene-28-oate **XLVIb**. While, replacing guanidine with

thiourea gave the corresponding methyl-2`-mercapto-18β-olean[3,2-d]-pyrimidine-12-ene-28-oate **XLVII** and methyl-2`-mercapto-6`-methyl-18β-olean[3,2-d]-pyrimidine-12-ene-28-oate **XLVIIb**.

IR spectrum of compound **XLVIb** shows NH_2 at 3438 cm^{-1}, while IR spectrum of compound **XLVIIa** shows SH at 3223 cm^{-1}. ^{1}H-NMR spectrum of compound **XLVIa** revealed NH_2 & pyridyl protons resonating at 3.6 and 6.91 ppm, while ^{1}H-NMR spectrum of compound **XLVIIb** revealed SH and $COOCH_3$ protons resonating at 2.85 and 3.31 ppm. EI-MS spectrum of compound **XLVIb** showed M^+ at m/z 533 (47%) [$C_{34}H_{51}N_3O_2$]. EI-MS spectrum of compound **XLVIIa** revealed M^+ at m/z 536 (57%) [$C_{34}H_{48}N_2O_2S$].

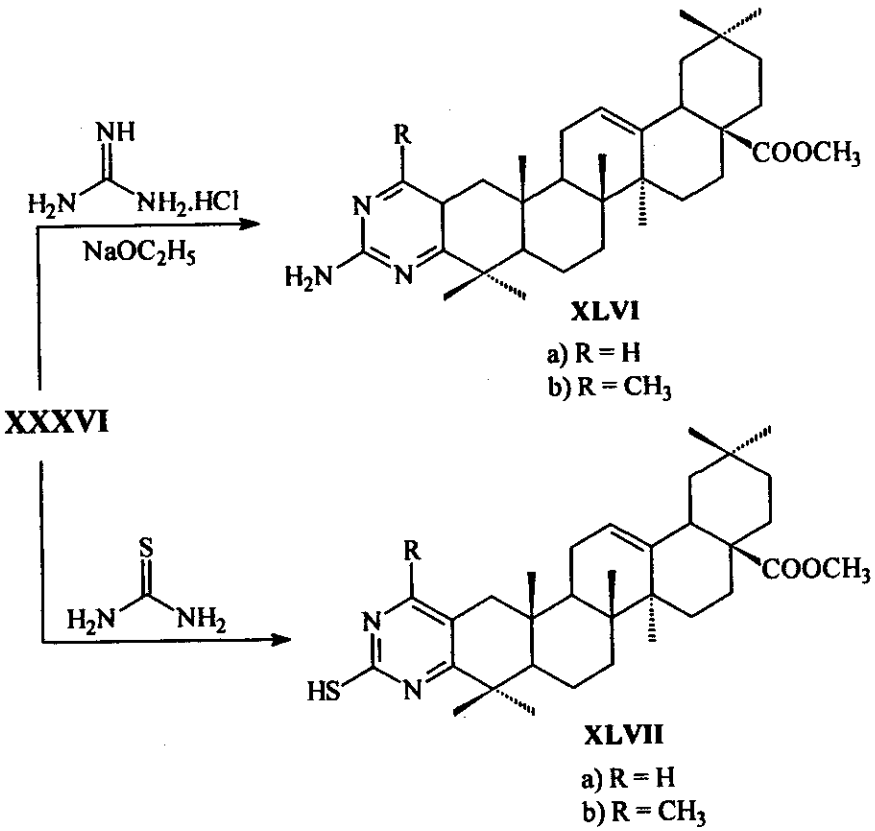

The reaction of guanidine with derivatives **XXXVI** probably takes place according to the following mechanism.

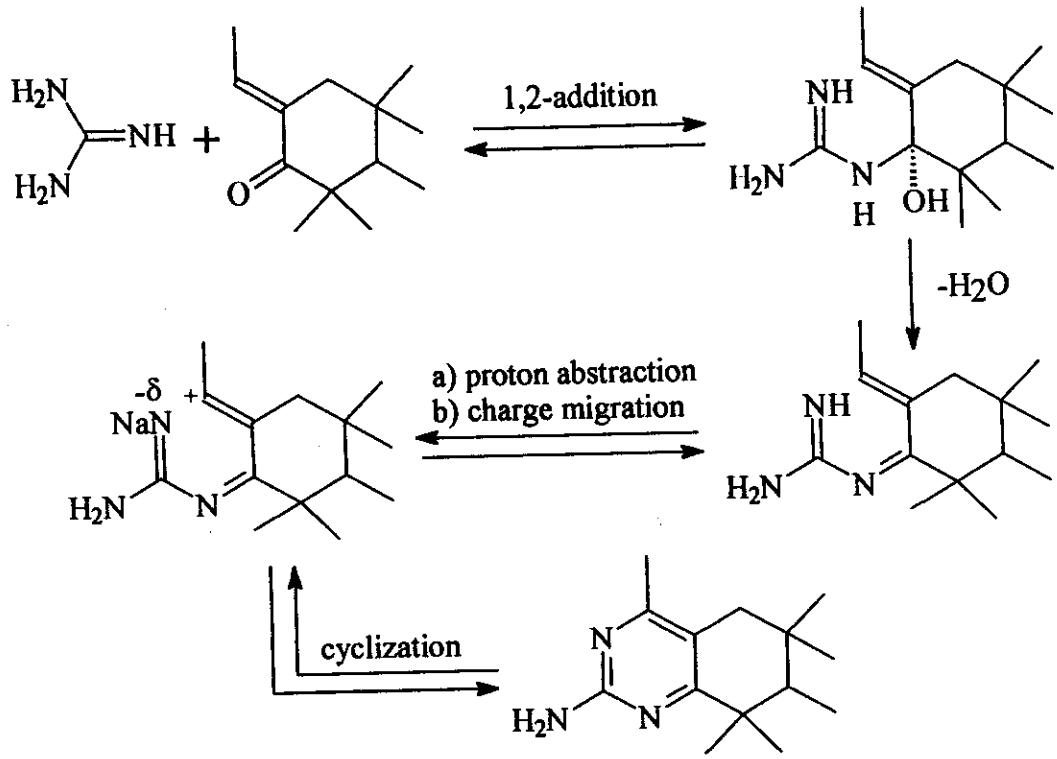

The reaction of thiourea with derivatives **XXXVI** probably takes place according to the following mechanism.

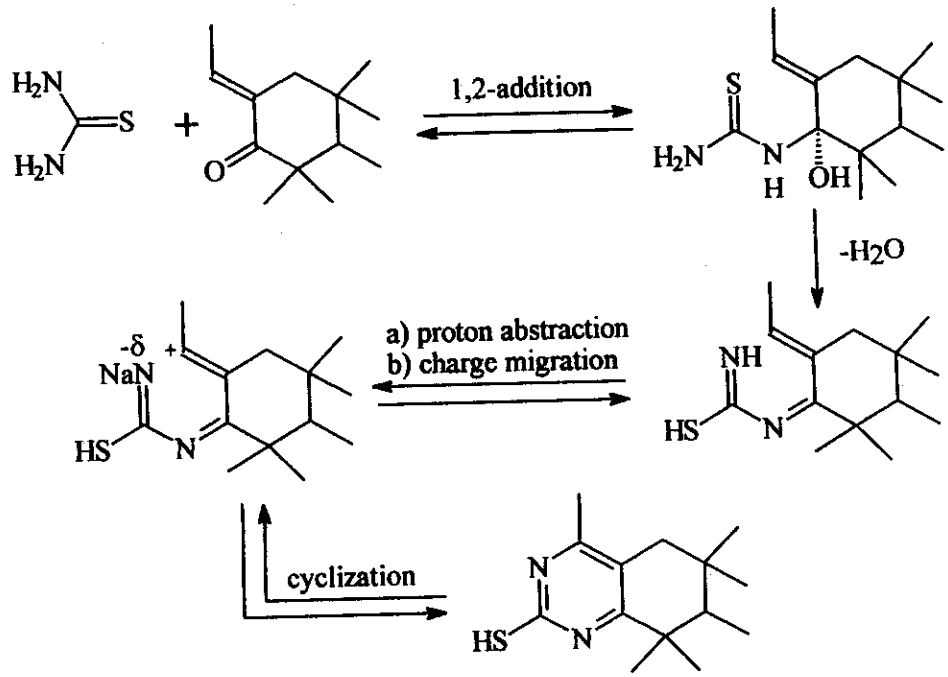

4.3.2. BIOLOGICAL ACTIVITY :

The synthetic design[82,83,129] to build up a new anti-inflammatory olean profile depends on the previous published data that

1- C-30 anilids and esters of glycyrrhetic acid have analgesic activities.
2- Cortecosteroids with Δ^1-ene showed increased anti-inflammatory activities.
3- Constriction of C-2 olean derivatives markedly increase the potency and duration of action of olean derivatives nearly to 200% than that of glycoconteroids.

So the author carried out the following modifications to attain new anti-inflammatory structure profile

- Replacement of C-30 with C-28 COOH to build new phenolic esters and anilides
- More D1-ene analogues
- Building up new heterocyclic fused ring systems to ring A.
- More modification at ring C.

So to achieve that, the author resorted to oleanolic acid as a molecule of choice serving the previously mentioned aim.

The study of the anti-inflammatory activities of some representative examples of the newly synthesized derivatives indicated.

6) Fusion of pyrimidine nucleus (two heteroatom six membered ring system) to ring A extensively increase the anti-inflammatory activities.

4.3.2.1 Structurel activity relationship of anti-inflammatory agents

- C-2 linked moiety, C-1 methyl and C-2 carbonyl decrease the anti-inflammatory activities.
- Anilides and phenolic esters at C-28 increase markedly the anti-inflammatory activities.
- One heteroatom six memebered fused to ring A system decrease the anti-inflammatory activities.
- Fusion with another cyclohexanone or two heteroatoms six membered ring system will increase the anti-inflammatory activities.

The strong biological rational adopted for the synthetic strategies adopted for synthesis of the newly prepared products is that concluded in previous published work[129-130] on glycyrrhetic acid, that mentioned that anti-ulcerogenic activities need a modification on ring A with no ester or amide formation at C-30.

So the author resorted to the following designs to enhance the anti-ulcerogenic activities

a) Construct a new heterocyclic ring system into ring A of olean skeleton in deferent fusion manner.
b) Abolish C-30 carboxyl's that is ulcerogenic (freely of reacted).

The C-30 olean skeleton provides this structural requirement is oleanolic acid.

The study of some representative examples of some of the newly synthesized compound revealed that.

1) C-2 confined ring A derivatives of oleanolic acid with C-1 methyl and C-28 methyl esters showed high anti-ulcerogenic activities as recalled for compounds XXIIa, XXIIIb and XXIVa (the highest potency is reported for compound XXIIa which is the benzylidene derivatives).

2) Removing the ester group at C-28 abolish the antiulcer effect as recalled for compounds XXVb, XXVc, XXVIIb due to the free carboxyl will interfere with muncin formation.

3) Abnormal and contrary to the previous study conclusion that state a that C-30 olean ester and anilide are ulcerogenic agent. Yet for the C-28 and esters and anilide are potent ulcerogenic as recalled for both compounds XXXIV and XXVe the high potency is for phenolic esters XXIVe due to the absence of the acidic character of anilides that alter mucin formation.

Construction of one six membered heteroatom fused ring A of oleanolic acid very extensively increase the anti-ulcer activities as for compounds XXVIIIa, XXIXb, XLb, XLa, XLIIa, XLIIIa. The highest

potency is for the XLIIb and XLIa) this is due to the pyridine structure (structure resemblance to proton pump inhibitor).

- Construction of a cyclohexanone ring system to ring A of oleanolic acid greatly increase the anti-ulcerogenic activities as for compounds XLIVa and XLVa.
- Construction of a two hetero atom fused ring system to ring A of oleanolic acid greatly increase the anti-ulcerogenic activities.

Sstructural activity relationship :

- C-2 confined ring system is essential for the anti-ulcerogenic activities with C-28 ester .
- Fusion of six membered ring system to ring A very extensively increase the anti-ulcerogenic activities, but pyridine nucleus has the greatest effect due to its resemblance to the PPI structure profile.

Finally our main non-clarified aim is looking for anti-ulcerogenic activities a property long-sought since most NSAJPS cause ulcerogenic effect upon medium term use (3-6 months). This goal achieved with compounds XLIVa, XLVa, XLVIa and XLVIIa that combine high anti-ulcerogenic and anti-inflammatory activities. These compounds contain another cyclohexene or two heteroatom six membered ring system fused to ring A of oleanolic acid .

Structural activity relationship :

Fusion of either cyclohexenone or two heteroatom six memebered ring system is essential for agents combining both anti-inflammatory and anti-ulcerogenic activities.

Table

Comp. No	% weight of paw edema	% Protection	Plasma PGE2 / ml	% inhibition PGE2	Ulcer index fo comp. + indomethacin		
Control	60.593 ± 1.867	-	7.95^{a} ± 0.49		-		
Indomethacin	13.865* ± 0.828	77.11	3.10^{a} ± 0.56	60.90	20		
XXIIa	33.945^{*a} ± 1.316	43.97	5.91^{*a} ± 0.76	25.47	16		
XXIIIb	30.981^{*a} ± 1.216	48.86	5.10^{*a} ± 0.77	53.68	13.53		
XXIVa	28.614^{*a} ± 1.315	52.77	4.13^{*a} ± 0.61	47.91	12.46		
XXVb	26.707^{*a} ± 1.094	55.92	4.25^{*a} ± 0.76	46.40	18.65		
XXVIc	33.603^{*a} ± 1.414	44.54	5.88^{*a} ± 0.491	25.85	19.87		
XXVIIb	37.81^{*a} ± 0.949	37.60	6.91^{*a} ± 0.491	12.86	19.47		
XXXIVe	22.816^{*a} ± 0.707	62.34	3.91^{*a} ± 0.321	50.69	11.14		
XXVe	21.314^{*a} ± 0.814	64.82	3.67^{*a} ± 0.341	53.72	15.61		
XXXVIIIa	19.613^{*a} ± 0.919	67.63	3.55^{*a} ± 0.342	55.23	7.4		
XXXIXb	40.707^{*a} ± 0.777	32.81	7.13 ± 0.67	10.08	4.6		

Table: (Cont.)

Comp. No	% weight of paw edema	% Protection	Plasma PGE2 / ml	% inhibition PGE2	Ulcer index fo comp. + indomethacin		
XLb	35.609*a ± 0.919	41.23	6.00 ± 0.819	24.83	5.8		
XLIa	45.00 ± 1.789	25.73	7.77 ± 0.68	2.01	4.7		
XLIIb	40.316 ± 1.918	33.46	7.00 ± 0.71	11.72	3.8		
XLIIIa	43.607 ± 1.618	28.03	7.83 ± 0.89	1.26	4.7		
XLIVa	17.608*a ± 0.543	70.94	3.38 ± 0.312	57.37	5.8		
XLVa	16.809*a ± 0.215	72.25	3.29 ± 0.222	58.51	6.7		
XLVIa	13.603*a ± 0.628	77.55	3.00 ± 0.167	62.16	6.7		
XLVIIa	14.668*a ± 0.524	75.79	3.08 ± 0.167	61.16	6.8		